Polymer Vol. 39 No. 19, pp. 4541–4559, 1998

0032-3861/98/$19.00+0.00

PII: S0032-3861(97)10306-8

Metastability and order in linear, branched and copolymerized polyethylenes

Vincent B. F. Mathot*, Rolf L. Scherrenberg and Thijs F. J. Pijpers
DSM Research, P.O. Box 18, 6160 MD Geleen, The Netherlands
(Received 17 July 1997; revised 29 September 1997; accepted 24 October 1997)

The melting behaviour of narrow-molar-mass-distribution fractions of linear polyethylenes during commonly used dynamic cooling and heating procedures – due to reorganization processes – shows barely any relationship with their crystallization behaviour during normal dynamic cooling. When short chain branching (SCB) is introduced, as in for example HDPE and LDPE fractions, the effects become smaller but they do not disappear. Measurements show that besides known influences such as thermal history and SCB, the chain length also has a considerable influence on the crystallization behaviour. For homogeneous and heterogeneous copolymers with large variations in comonomer content the crystallization behaviour, morphology and melting behaviour were studied in relation to the chain macro- and microstructure. In homogeneous ethylene copolymers, the morphology changes considerably as the comonomer content increases: at low comonomer contents folded-chain crystallization in a lamellar base morphology prevails, with the lamellae usually being organized into spherulitic superstructures. At higher comonomer contents, the crystallite thickness decreases and the lateral dimensions become smaller, until ultimately there is folded-chain crystallization in a granular base morphology without any organization into superstructures. At the highest comonomer contents, experiments and Monte Carlo simulations point to a fractal growth type crystallization, where clusters of 'loosely packed ethylene sequences' are formed. Both d.s.c. and real-time SAXS yield detailed information for all copolymers, even for the virtually amorphous copolymers which crystallize and melt just above the glass transition temperature. Even in a homogeneous copolymer, several of the above-mentioned morphologies can occur side by side due to the ethylene sequence length distribution in the polymer. In heterogeneous copolymers such as LLDPE and VLDPE, practically all of the above-mentioned morphologies can be found in one and the same sample.

(Keywords: chain microstructure; crystallization; heterogeneous copolymer)

INTRODUCTION

Classification of polyethylenes

Figure 1 shows a classification of the most important commercial polyethylene types[1] according to density or crystallinity at room temperature. The ranges indicated are to a large extent determined by variations in molecular structure. Two important parameters have a great influence: in the first place the chain length and the chain length distribution and secondly the type, number and distribution of (short) branches of the backbone chain. The short branches in existing polyethylenes have in common that they hinder the crystallization of crystallizable ethylene units. The number of branches and the distribution thereof are reflected in the ethylene sequence length distribution. However, even at the same distribution the degree of hindrance may differ, depending on the nature of the branch.

Besides these macrostructural and microstructural parameters, sample conditions and the presence of other components may also influence the crystallization behaviour and give rise to the ranges listed in *Figure 1*. Examples of influences during processing are: pressure, orientation, the solvent used, the presence of other polymers and additives. The thermal history of the polymer, in particular the cooling rate, is also very important. This is often to a large extent imposed by the processing technique used.

Polyethylenes are a commercial success not only because the raw materials on which they are based are readily available but also because they offer excellent opportunities for varying the chain macro- and microstructure in combination with a wide range of processing techniques. Many new types have been developed over the years, and the possibilities have by no means been exhausted. The first type, low density PE (LDPE), was developed in the 1930s, followed by high density PE (HDPE), rubbers such as ethylene–propylene terpolymers (EPDM), linear low density PE (LLDPE) and very low or ultra-low density PE (VLDPE or ULDPE). Currently a lot of work is being done on the development of homogeneous copolymers, made possible by the use of metallocene catalysis[2,3]. Ethylene–propylene (EP), ethylene-1-butene (EB), ethylene-1-hexene (EH) and ethylene-1-octene (EO) copolymers have already been introduced in the market. It is to be expected that the number of comonomer types will still increase substantially. Polyethylenes with special branched structures are also receiving a lot of attention.

Clearly, the days when the term 'polyethylene' referred to a single polymer are long past: the term covers a class of ethylene-based polymers having widely differing structures and properties[4].

EXPERIMENTAL

Materials

Sample data are given in *Table 1*. For samples not mentioned in the table, see references given in the text.

* To whom correspondence should be addressed

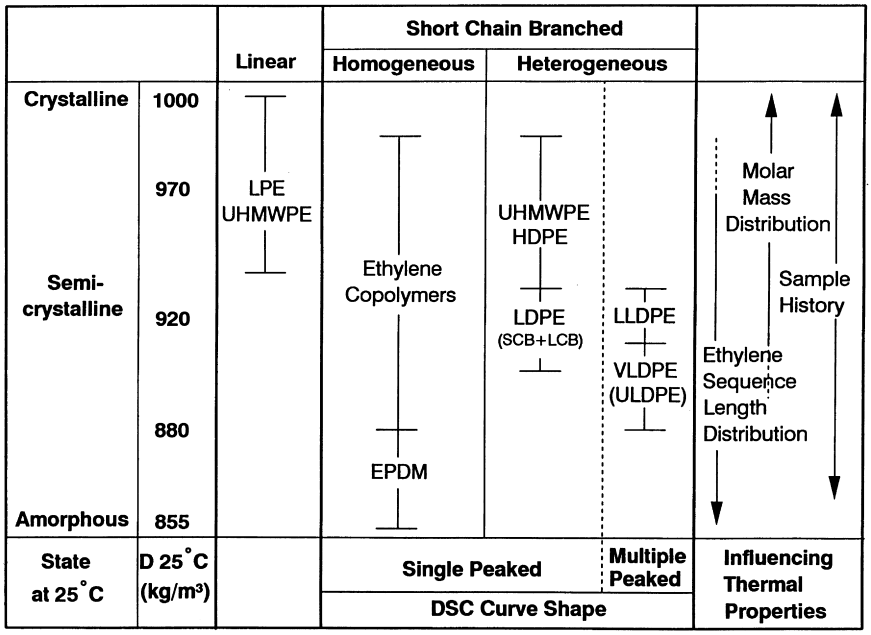

Figure 1 Classification of important polyethylene types according to density at room temperature, chain structure, DSC curve shape and parameters influencing the crystallization and melting behaviour

Table 1 Codes, molecular structure data and densities of some linear polyethylenes, homogeneous ethylene–propylene copolymers, and homogeneous and heterogeneous ethylene-1-octene copolymers

Ethylene based polymer	Sample code	Comonomer	D^{23C} (kg/m^3)[a]	X_e (mol%)[b]	M_n^* (kg/mol)[c]	M_w^* (kg/mol)	M_z^* (kg/mol)
LPEs	JW1114	—	n.d.	100		52	
	LPE-3[d]	—	see *Figure 5*	100		120	
Homogeneous EO copolymers	JW1116	C8	n.d.	97.9		47	
	JW1120	C8	n.d.	94.8		31	
	PEO-5	C8	n.d.	94.5		345	
	JW1121	C8	n.d.	92.0		34	
	JW0103	C8	n.d.	90.2		46	
	EO V[e]	C8	872	88.5	130	240	380
	EO M[e]	C8	870	87	42	91	150
Homogeneous EP copolymers	EP 207	C3	896	89.4	39	120	220
	EP 203	C3	n.d.[f]	82.6	25	170	320
	EP 198	C3	n.d.	69.2	105	270	470
Heterogeneous EO copolymers	VLDPE	C8	902	93.8	22	95	320
	VLDPE	C8	888	91.5	15	84	380

[a] The densities were determined on compression-moulded plates
[b] Mole percentage incorporated ethylene units
[c] The M^* values (asterisked to indicate that use was made of the conventional calibration) were determined with the aid of SEC at approx. 140°C using 1,2,4 TCB as solvent
[d] NBS SRM 1484
[e] V and M: vanadium- and metallocene-based, respectively
[f] Not determined

Information about the LPEs, the HDPE and the LDPE in *Figures 2*, and *4* can be found in ref.[4].

Instrumentation

DSC. The measurements were performed using Perkin–Elmer differential scanning calorimeters. The measuring block and the glove box surrounding it were flushed with very dry nitrogen. The temperature calibrations in heating were made with the aid of the melting temperatures of pure indium and lead at the scan rates used. The temperature correction for cooling rates was performed by mirroring the corrections obtained in heating for indium using an extrapolation to zero scan rate. The energy calibration was performed using the melting enthalpy of indium and was checked via c_p measurements of sapphire in the range measured. Measurements were performed on the copolymers in one step according to the so-called continuous measurement procedure[5] in the temperature ranges indicated and at the scan rates indicated. The cooling curves and second heating curves were recorded. From a signal measured—caused by pan plus sample—the (previously measured) signal of the empty pan was subtracted. In-house developed software was used for measurement and evaluation.

TEM. In the d.s.c. apparatus the copolymers were cooled at 10°C/min or 5°C/min from temperatures between

150 and 200°C. After cooling to about −120°C and trimming at that temperature, the samples were stained with chlorosulphonic acid vapour to enhance the contrast between crystalline and amorphous regions. TEM studies were performed on coupes with a thickness of about 100 nm or about 70 nm using a Philips CM 200 TEM at 120 kV. $HClSO_3$ staining produced better results than staining with RuO_4. Ruthenium tetroxide has been found to be too aggressive for the copolymers: the lamellae are thinner, probably because they are attacked by RuO_4, while they may be poorly visible due to the grainy structure of the pictures as caused by RuO_4.

SAXS–WAXS. Simultaneous SAXS–WAXS–d.s.c. measurements were performed on beamline 8.2 of the SRS at the SERC Daresbury Laboratory, Warrington, UK. The pin-hole camera was equipped with a multiwire quadrant detector (SAXS) located 3.5 m from the sample position and a curved knife-edge detector (WAXS) that covered 120° of arc at a radius of 0.2 m. The scattering pattern from an oriented specimen of wet collagen (rat-tail) was used to calibrate the SAXS detector and the reflections of an LLDPE were used to calibrate the WAXS detector. For a detailed description of the storage ring, radiation and camera geometry and data collection electronics, see ref.[6].

The frames were taken at intervals of 1 and 2°C for the scan rates of 10 and 20°C/min respectively. The experimental data were corrected for background scattering, sample transmission and the positional non-linearity of the detectors. A measure of the variation of the crystallinity of copolymer EP 207 as a function of temperature was obtained by determining the integrated intensity of the WAXS 110 reflection after subtracting the amorphous contribution. For this purpose, the WAXS patterns of the copolymer EP 198 were used after applying the same thermal treatment. In this way, the shift of the amorphous pattern with the temperature could be taken into account. The influence of the comonomer content is small[7]. The SAXS and WAXS patterns obtained were brought to an absolute scale via an external calibration at room temperature. For this purpose, the samples were given the same thermal history as during the synchrotron experiments. Subsequently, the samples were measured at room temperature on an Anton Paar Kratky type SAXS camera and a Philips PW1820 Bragg–Brentano type goniometer. The absolute SAXS intensity of the sample was determined using a Lupolen standard, supplied with the Kratky camera. The absolute WAXS crystallinity was obtained by applying Ruland's method using a computer program developed by Vonk[8].

RESULTS AND DISCUSSION

Metastability of linear and branched polyethylenes

Crystallization and melting temperatures. It has been demonstrated many times that linear polyethylenes (LPE) exhibit a large degree of metastability, see Keller[9] for a recent discussion. The mere fact that perfect crystals with maximum dimensions in which the chains are extended (the kind of crystals one would expect on thermodynamic grounds) are obtained only under special conditions[10,11] indicates that the crystallization process is far from ideal and that the resulting crystals will be metastable, especially if the growth rate of the metastable crystals exceeds that of the stable crystals[9,12]. This means that there will virtually always be a tendency towards the thermodynamic equilibrium situation. In practice this means that under conditions which tend to increase chain mobility changes in morphology are likely to occur.

Such changes occur more often than one would expect. The fact that relatively little is known about the metastability phenomenon is due to the lack of fully developed methods for monitoring changes under certain desired conditions. Only recently has it become possible to carry out extensive research with the aid of high-intensity synchrotron X-ray sources. This includes the possibility of carrying out 'dynamic'—time-resolved—measurements and comparing them with 'static' measurements (often very time-consuming measurements, for example isothermal measurements at a chosen temperature or measurements at room temperature after annealing at a higher temperature). By means of synchrotron measurements it is possible, for example, to monitor changes in the long period at high temperatures or in temperature scanning. In this way not only the final state of the material but also the process of getting there are mapped in a very targeted and detailed manner. Another, less well-known example of metastability is the following: in density measurements at room temperature on copolymers having high comonomer contents it is common practice to follow special procedures to 'stabilize' the density (and hence the crystallinity). The density measurement is sensitive enough to monitor small changes in the amorphous and crystalline fractions.

This information shows that under specific circumstances (including conditions occurring in practice) polyethylene undergoes changes in terms of morphology and properties. A well-known phenomenon observed during heating is recrystallization at a high temperature. Still, it is common practice among researchers to interpret the d.s.c. melting curve and the associated characteristic quantities such as peak temperature in absolute terms. Many researchers even prefer melting curves to crystallization curves; they reason that crystallization is to a large extent kinetically determined (because of the nucleation process), in contrast with melting. This idea is partly supported by the fact that melting does not require a nucleation process[13]. On the other hand, it is a well-known fact that while crystallization curves are strongly influenced by the cooling rate, melting curves are heavily influenced by the cooling rate and the subsequent heating rate. Although d.s.c. offers special facilities (in Perkin–Elmer d.s.c. the cooling and heating rates can be controlled reasonably well up to about 150°C/min and a few hundred degrees per minute, respectively) it offers insufficient possibilities for studying recrystallization in detail. The reorganization processes sometimes proceed so rapidly that even the above-mentioned scan rates are too low to study, e.g. recrystallization in detail, let alone to prevent this process. A partial solution might be provided by the scanning adiabatic calorimeter, which enables heating rates of up to 36 000°C/min[14–16]. Other – but generally rather laborious – methods for avoiding recrystallization via fixation of chains through crosslinking of molecules in the amorphous phase convincingly show that there will always be reorganization processes during heating, often already at a few tens of degrees below the theoretical equilibrium melting temperature. In other words: reorganization processes during heating are the rule rather than the exception. Only the degree to which they occur may vary; it is influenced by many factors, such as the thermal history, the temperature–time profile during heating but also the molecular structure, as will be discussed below.

Figure 2 shows a large number of factors that influence the crystallization and melting behaviour of LPE fractions with narrow molar mass distributions[17]. First of all it is clear that chain length is an important parameter which is often neglected or underestimated. At a cooling rate of 5°C/min, crystallization is increasingly hindered as the chain length increases, due to entanglements which prevent reptation of chain parts to the growth front. This causes the decrease in crystallization peak temperature with increasing chain length from approx. 20 kg/mol onwards. For the smallest chains, crystallization and crystal growth still fall within regime I[18], but from approx. 10 kg/mol onwards nucleation and crystal growth fall within regime II. From about 100 kg/mol onwards, the peak temperatures are constant. This is because, on account of multiple nucleation (regime III[19]) parts of the same chain are trapped in different crystal growth fronts (in the same crystal or in different crystals) so that the total chain length is no longer relevant. Incidentally, despite this constant crystallization temperature the degree of supercooling still increases because the melting temperature still increases slightly with increasing chain length. At lower cooling rates, there is less hindrance with increasing chain length. Since there is more time available for disentanglement, crystallization takes place at higher temperatures, that is, at lower degrees of supercooling. As a result, multiple nucleation is also reduced: there is a shift towards nucleation and growth in regimes II and I. Upon an increase in cooling rate the reverse occurs: a shift to higher degrees of supercooling and to regime III nucleation and growth. It is interesting to note that crystallization apparently takes place on a time scale corresponding to that of the d.s.c. conditions. Incidentally, the d.s.c. crystallization peak temperatures measured at cooling rates of 5°C/min are confirmed within one degree by light-microscopical measurements.

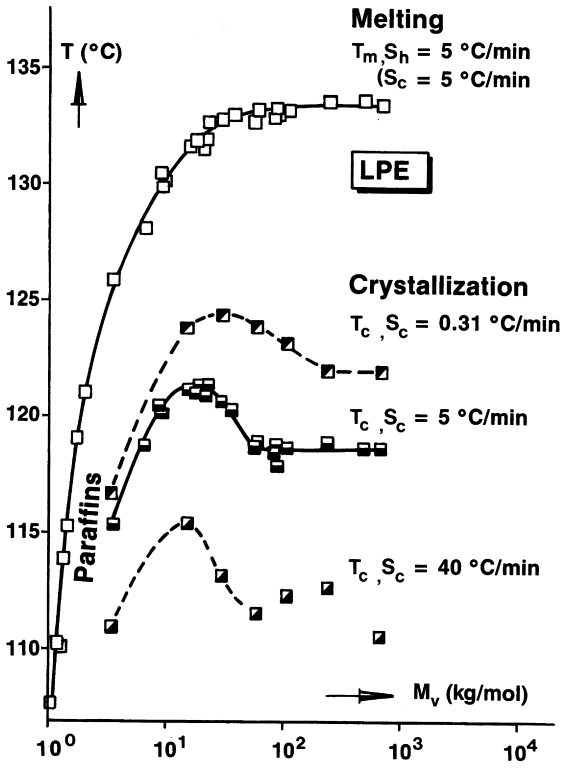

Figure 2 Crystallization and melting peak temperatures, T_c and T_m, respectively, for linear polyethylene (LPE) fractions with narrow molar mass distributions, as obtained from d.s.c. cooling and heating curves, and T_m for paraffins, as obtained from the literature, as functions of molar mass. Influence of cooling rate on T_c

However, the development of the melting peak temperatures with increasing chain length is at least as interesting. An increase in T_m with increasing M is what everybody expects, but there is no relationship whatsoever with the development of T_c. Few people know this, because they usually study only the melting behaviour and, although they do give a thermal history, fail to record the associated crystallization behaviour. It will be clear from *Figure 2* that

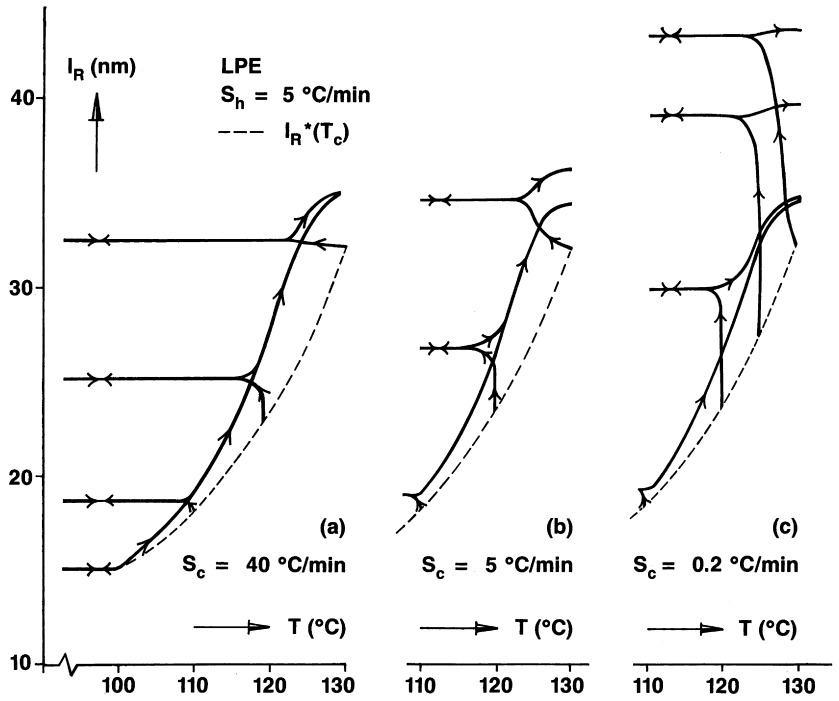

Figure 3 The Raman length (⟶), $l_R(T)$, for LPE as a function of the Raman length at the temperature at which the second stage of crystallization starts (— — —), $l_R^*(T_c)$; the cooling rate [(a) $S_c = 40$°C/min; (b) $S_c = 5$°C/min; (c) $S_c = 0.2$°C/min] and the subsequent heating rate ($S_h = 5$°C/min)

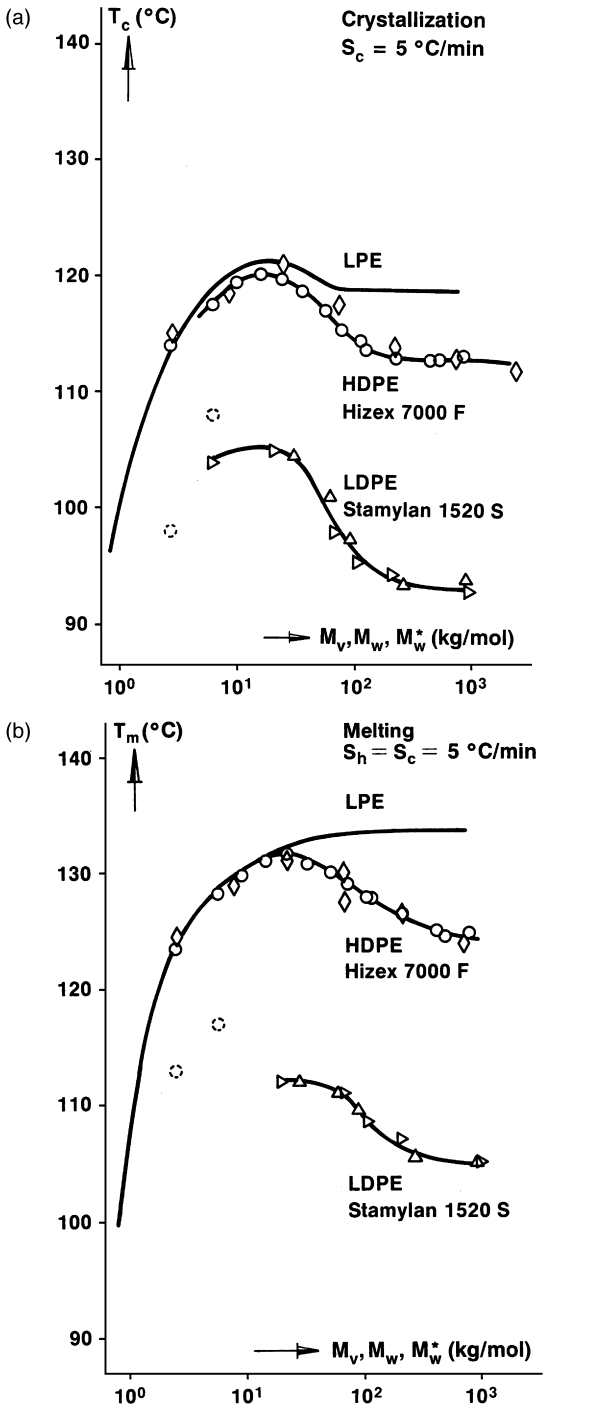

Figure 4 (a) Crystallization peak temperatures obtained in cooling at a rate of 5°C/min by d.s.c. for HDPE fractions (○, direct extraction; ◇, 'analytical' SEC) and LDPE fractions (△, preparative SEC; ▷, 'analytical' SEC) as functions of M_v, M_w and M_w^* for LPE, HDPE and LDPE, respectively. LPE curve according to *Figure 2*: (b) melting peak temperatures in subsequent heating at a rate of 5°C/min, otherwise as in (a)

somewhere between cooling and heating reorganization occurs on such a scale that the expected relationship between T_c and T_m is completely obscured.

Obviously, this has many consequences. For one thing, it is not to be expected *a priori* that any meaningful relationships will be found between T_c, the morphology at room temperature, and T_m. This means that Hoffman–Weeks[20] and Gibbs–Thomson[21] extrapolations will be impossible or very difficult because the crystal thickness is unlikely to be constant and therefore not unambiguously related to the T_m measured.

In *Figure 3* an attempt is made to explain this. It shows a simulation of the Raman length (the length of a chain segment incorporated into a crystal: if the angle with the longitudinal dimension of the crystal is constant, this is a measure of the crystal thickness) for LPE on the basis of isothermal experiments[22–24]. The figure shows the calculated influences of the crystallization nucleation temperature [the initial Raman length at T_c immediately after the formation of the crystallite nucleus, indicated by $l_R^*(T_c)$]; the cooling rate (in this case 40, 5 and 0.2°C/min) and a constant heating rate (5°C/min). It can be concluded that if, at a high temperature, the LPE is given time to reorganize, a considerable degree of reorganization can occur, resulting in an increase in the Raman length. This means that the crystal thickness can increase considerably *both in cooling and in heating*. As far as heating is concerned this should come as no surprise, but very few people seem to expect an increase in crystal thickness during cooling. As remarked earlier, synchrotron measurements confirm these phenomena: it even proves to be extremely difficult to determine the initial longitudinal nucleus dimension, $l_g^*(T_c)$, because the reorganization takes place very rapidly[25–28]. The figure also illustrates that the use of the Hoffman–Weeks relation is problematic because it assumes a fixed ratio between $l_g^*(T_c)$ and $l(T_m)$. In the figure it can be seen that this assumption is unlikely to be correct when T_c varies.

As noted earlier, molecular structure parameters also determine whether or not reorganization occurs and to what degree it occurs. In the case of LPE, reorganization will be made possible mainly by sliding diffusion[29,30] of chains through crystallites, one of the reasons being that in LPE loops, cilia, etc. occur, in particular at high degrees of supercooling during crystallization, for example at high molar masses and/or high cooling rates. In low-branched PE and in copolymers with low comonomer contents reorganization via sliding diffusion is difficult because short side chains are preferentially excluded from the crystal and will therefore be present mainly in the amorphous phase. These branches will not take part in the process of diffusion through the crystal. However, this hindrance may be limited because the ethylene sequence lengths are still so long that sequences will be folded many times in the crystallites, also with loops, etc. At very high comonomer contents (in the case of a fringed-micelle-type crystallization) the hindrance will be much greater. However, even in this case the ethylene sequences present, of which mostly only parts will be trapped inside crystallites (which means that there will still be crystallizable ethylene sequences at the crystallite surface) will still give rise to perfection and growth of the crystallites.

The fact that sequences are only partly trapped has to do with the non-equilibrium nature of the crystallization. For thermodynamic reasons, sequences of equal length will preferentially crystallize simultaneously[31–33], but this will in part be prevented by diffusion problems while moreover multiple nucleations will occur at the prevailing degree of supercooling. As a result, there will be no perfect matching of sequence lengths because a trapped sequence, even if its length is not exactly equal to that of adjacent sequences, will be fixed fairly quickly because sequences of the same chain which have already crystallized or which are crystallizing simultaneously will prevent it diffusing to a more optimum place in the same crystallite or to a different

crystallite. This means that sequences of unequal length will crystallize in the same crystallite, leading to a considerable number of loops, etc.[34]. If short side chains are included in the crystal (which can be the case if the short side chains are propylene units and to a lesser extent if they are 1-butene units) sliding diffusion is of course prevented very effectively. For the above-mentioned reasons, reorganization via sliding diffusion is less and less likely to occur as the comonomer content increases.

In *Figure 4* the curves for LPE from *Figure 1* have been included to enable a comparison with narrow-molar-mass-distribution fractions of a HDPE and an LDPE. In the HDPE, 1-butene was incorporated as comonomer (approx. $4CH_3$/1000C on average, density of compression moulded plate at room temperature 952 kg/m^3), the amount of incorporated 1-butene increasing with increasing molar mass. This partly explains the differences compared with the LPE curves at high molar mass values. However, the melting behaviour of the HDPE fractions is the most interesting. In contrast with LPE, the melting behaviour of the HDPE fractions is more or less analogous to their crystallization behaviour. This can only be explained if we assume that (as outlined earlier) the degree of reorganization (and hence the increase in melting peak temperature) is limited due to the presence of short chain branching (SCB).

The same figure also includes data for LDPE (approx. $20CH_3$/1000C on average, density of compression moulded plate at room temperature 922 kg/m^3). High pressure LDPE is a very complex polyethylene type whose short chain branching structure has not yet been unravelled. SCB with branches of different lengths occurs alongside long chain branching (LCB). With the aid of infrared measurements it was demonstrated for the various fractions that—after corrections for endgroups – the number of CH_3/1000C decreases slightly with decreasing M. So the decrease in both T_c and T_m cannot be due to an SCB content increasing with increasing M. The results show that the molar mass is responsible for the large decrease (approx. 10°C!) in T_c[35]. LCB does not play any role in the decrease because in non-LCB-containing polymers an analogous decrease has been observed[36–39]. LCB does play a role with regard to the M axis because on account of LCB an 'apparent' rather than an absolute molar mass is measured by SEC. The figure suggests that for different polyethylenes the decrease in T_c with decreasing molar mass manifests itself mainly between about 20 and 100 kg/mol (*apparent molar mass*) and that it is the apparent molar mass, M^*, rather than M which is the most important parameter in crystallization. This suggests that the molecular dimension in the melt (which is related to the molecular dimension in solution as measured by SEC, resulting in an apparent molar mass, M^*) is the real parameter in crystallization. So besides SCB, the molar mass and (indirectly) LCB are also important parameters governing crystallization.

In the case of LDPE the fact that SCB limits the opportunities for reorganization follows from the fact that the melting peak temperatures as a function of M are analogous to the crystallization peak temperatures. However, in absolute terms the decrease with decreasing M during melting is about half the decrease during crystallization; this suggests that reorganization is not prevented. Another clue pointing in this direction is that $T_c(M^*)$ is highly sensitive to differences in cooling rate, whereas $T_m(M^*)$ is not. The fraction with $M_w^* = 250$ kg/mol, for example, shows a decrease of five degrees in T_c when the cooling rate decreases from 5 to 0.31°C/min. Upon subsequent heating at 5°C/min, however, the increase in T_m is less than one degree. This must be due to the fact that the ethylene sequences in the crystallites are still folded many times.

The kinetic determinacy of crystallization and melting and the resulting metastability of the phases has been illustrated above with reference to the influence of parameters such as SCB, molar mass and cooling rate. The influences of SCB and cooling rate on melting behaviour have been studied extensively for many years. However, only recently a start has been made on the systematic study of the influence of the molar mass. Unfortunately, quantitative d.s.c. data are generally lacking, and it is precisely this technique which is eminently suitable for studying the kinetics of the processes involved. So a full analysis is still being awaited. In addition, much more attention should be paid to the study of crystallization behaviour under dynamic conditions, such as during cooling, combined with the subsequent melting behaviour. In such studies the cooling and heating rates should be systematically varied. Preferably, techniques should be developed which enable much higher (controlled) cooling and heating rates. This would make it possible to study the kinetics of the forming of metastable phases much more effectively. Moreover, reorganization effects would be prevented and a link would be achieved with real processing conditions.

Crystallinity. Apart from crystallization and melting temperatures, the fractions of the metastable phases are also important. Traditionally, the two-phase model has been used for PEs: a sample is thought to consist of crystalline and amorphous phases. Of course, there will be an interface between these phases about which e.g. SAXS can provide information. As to whether a third phase, for example a 'rigid amorphous' or 'hindered amorphous' phase, is present in any measurable quantities is still the subject of study and debate. The reason why this question has not been resolved yet is that this fraction, if it is present, is small, in contrast with other polymers such as PEN[40], PBT[41], etc. This is due to the fact that the PE chains are very flexible. In semi-crystalline polymers, the expression 'rigid amorphous' mainly refers to chain segments which are not located in crystallites (which means their mobility is not really low) but which do not have the increased mobility of the amorphous phase either. This concerns parts of a chain which are in both the crystalline and the amorphous phase and which, as far as their mobility is concerned, are strongly correlated so that the mobility of the chain part in the amorphous phase is to a large extent determined by the crystalline phase. The reduced mobility may give rise to a phase with a vitrified character, that is, vitrified at temperatures which are higher (in some polymers up to 100°C higher) than the glass transition of the 'mobile' or 'unhindered' amorphous phase. For a discussion see ref.[42].

Such a third phase can be modelled as far as its enthalpy and heat capacity are concerned. For most polyethylenes this does not seem to be very meaningful, except perhaps for ultra-high molecular weight PE (UHMWPE). Any anomalies which have been attributed to a third phase can usually be traced back to non-quantitative measurements and incomplete analyses. For example, the d.s.c. crystallinities reported in the literature are virtually always based on non-quantitative d.s.c. curves and are evaluated using arbitrary methods. This can easily produce absolute errors of 10%[43], which are of the same order of magnitude as the

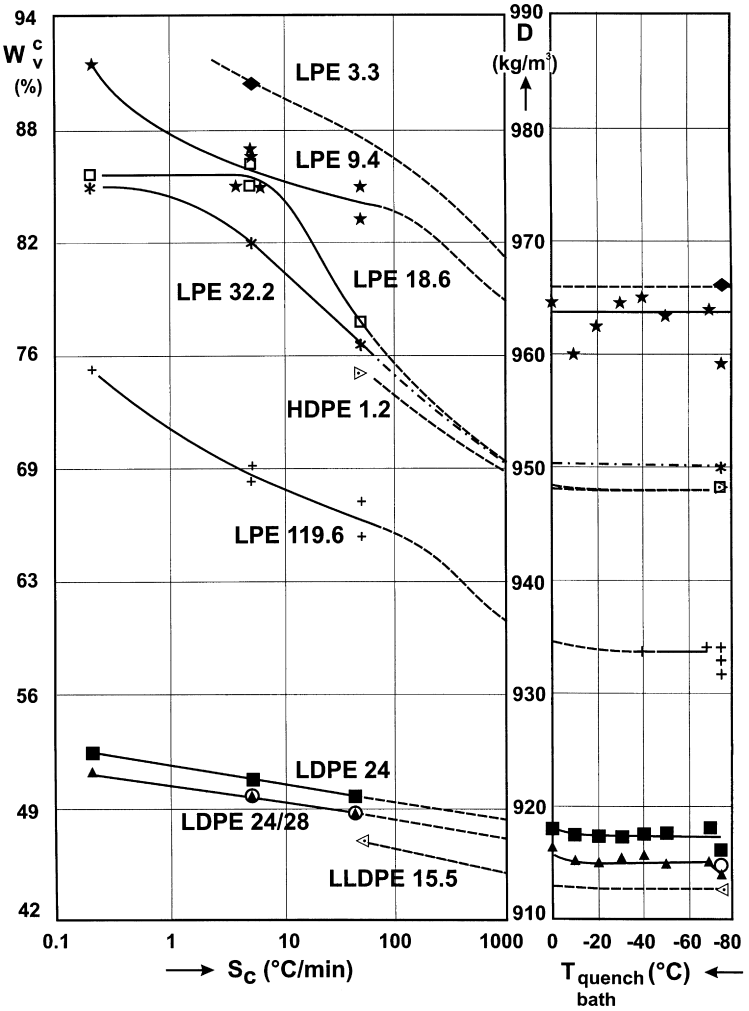

Figure 5 The influence on overall density and volume-based mass crystallinity at room temperature of molar mass and cooling rate for LPEs (numbers indicate M_v in kg/mol) and of cooling rate for a HDPE, two LDPEs and a heterogeneous LLDPE (numbers indicate CH_3/1000C)

differences in crystallinity measured by different methods. In order for the analysis to be correct, it should preferably be based on heat capacity measurements (although an alternative method is available[44]) followed by a straightforward evaluation with the aid of a two-phase or three-phase model. The two-phase model has been adequate so far and the d.s.c. results are in agreement with an evaluation of density measurements using the two-phase model[45].

Figure 5 shows densities and the mass crystallinities at room temperature calculated from them for LPE (with variation in *M*), a HDPE, two LDPEs and an LLDPE as a function of the cooling rate and in case of quenching. For LPE it can be seen that an increase in molar mass (from 3.3 to 119.6 kg/mol, the sample with the highest molar mass is NBS SRM 1484) causes the crystallinity to drop by about 20% (absolute), which is in accordance with literature data. SCB has a considerable influence on the crystallinity: for the samples shown here, when going from LPE to LDPE the crystallinity decreases by about 30%. The cooling rate (for the range between 0.3°C/min and quenching) also has a considerable influence on the crystallinity: a comparison of the LPEs and HDPE shows a variation in crystallinity of about 16%. In the case of the LDPEs and the LLDPE the variation is smaller: approx. 6%. In summary, it can be concluded that SCB, molar mass and cooling rate affect the crystallinity in a major way.

Much more attention should be paid to the quantitative measurement of the fractions of the (metastable) phases present as a function of temperature and time, for example the fractions of crystalline, amorphous and possibly rigid amorphous material or any other phases present. As far as this is concerned d.s.c. is a very promising technique, because it provides an easy way of obtaining temperature–time profiles enabling the kinetics of processes to be studied – sometimes on the time scale of the processes themselves. This does, however, require quantitative measurements for determining enthalpy changes, for example as based on heat capacity measurements. Unfortunately, the *calorimetric potential of d.s.c.* is hardly ever utilized because enthalpy changes are often measured in an arbitrary manner. This means that in many cases only the temperatures at which phase changes occur are quantitative (while the measurements are moreover mostly carried out in heating, which means that often only melting and devitrification are studied), so that d.s.c. is in fact used as a very expensive thermometer. Besides carrying out quantitative measurements, one should preferably use the two-phase model in evaluating the enthalpy changes. Three-phase models need to be developed further: for various non-PEs the two-phase model is inadequate. Finally, time-resolved WAXS and SAXS synchrotron measurements are very promising techniques when it comes to providing insight into the metastability of phases and into the phases themselves. Examples of this will be given in the following sections.

Homogeneous copolymers[46,47]

First of all, the term 'homogeneous' as applied to copolymers needs to be explained. It is here understood to refer to single-site copolymerization in which the statistics of ethylene and comonomer addition can be unambiguously characterized by a single set of reactivity ratios. Copolymers with different comonomer contents can be obtained by varying the ethylene/comonomer ratio in the reactor at the catalyst site. In addition, the addition statistics are assumed to be independent of the chain length. Various catalyst systems, including metallocene catalysts, meet these criteria. Others, such as the Ziegler–Natta catalysts used in the production of LLDPE and VLDPE, do not.

The fact that homogeneous catalysts have a single active site means that the ethylene sequence length distribution is single-peaked. Under normal cooling conditions the crystallite dimension distribution also appears to be single-peaked, resulting in a single-peaked melting temperature distribution, see *Figure 1*. On the other hand, a single-peaked melting temperature distribution need not imply homogeneous comonomer or SCB incorporation, see HDPE and LDPE in *Figure 1*: these are definitely not homogeneous. Multiple-peaked crystallization and melting temperature distributions are generally associated with heterogeneous comonomer incorporation, which may for example be due to the presence of multiple active sites as in the case of LLDPE and VLDPE.

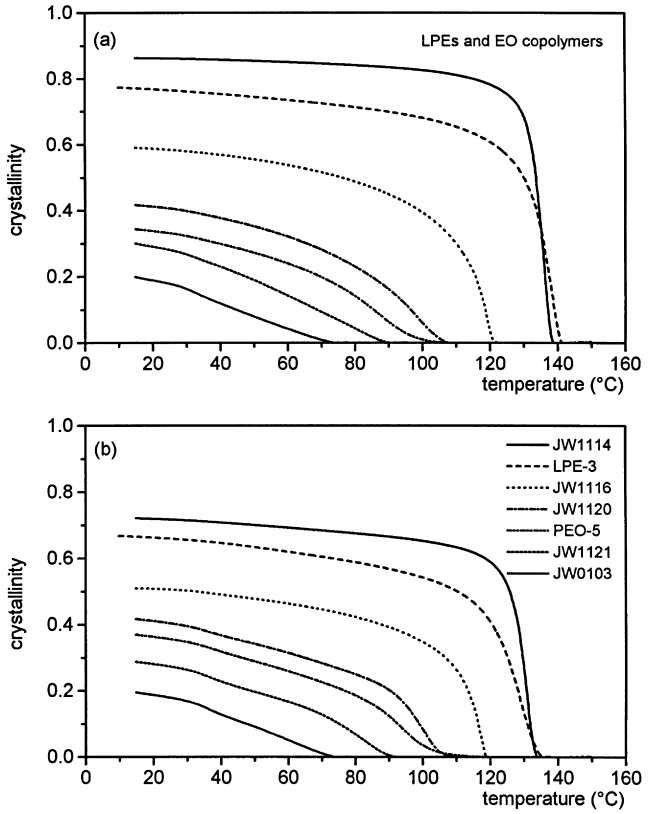

Figure 6 Enthalpy-based mass crystallinity curves for two LPEs and some homogeneous ethylene-1-octene copolymers based on d.s.c. heat capacity measurements in heating at 5°C/min after cooling at 0.1°C/min (a) and after quenching in liquid nitrogen (b)

Homogeneous copolymers with densities above about 870 kg/m^3. *Figure 6* shows crystallinity curves obtained in heating from room temperature for slowly cooled and quenched LPEs and homogeneous ethylene-1-octene copolymers. The curves were obtained by integrating d.s.c. heat capacity curves and comparing the results with the reference values for LPE[48,49]. The great influence of the comonomer content is visible. In addition, the LPEs and the copolymers with the lowest octene contents appear to be strongly influenced by the cooling rate: the absolute differences range from 10 to 15%. By contrast, the crystallinities of the copolymers with the highest octene contents are virtually equal. However, to complete the picture, measurements need to be carried out at lower temperatures as well, preferably starting at the glass transition temperature (for JW0103, for example, this would be from about −50°C). As will be shown below, the (maximum) crystallinity at the lowest temperatures can be considerably higher than that at room temperature. This means that at room temperature the samples with the highest octene contents still contain plenty of material that can crystallize below that temperature. Changes in copolymer density during

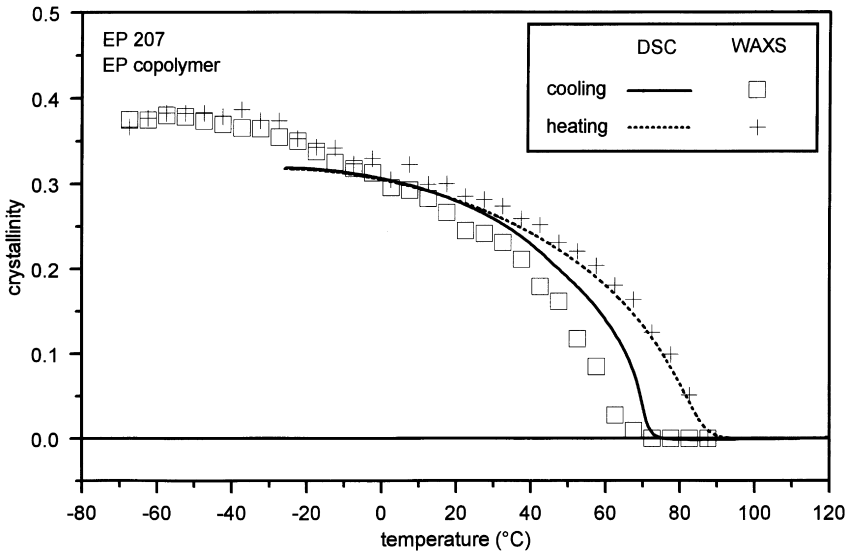

Figure 7 Enthalpy-based mass crystallinity curves based on d.s.c. heat capacity measurements and mass crystallinity curves from WAXS for cooling and subsequent heating at 10°C/min for EP 207

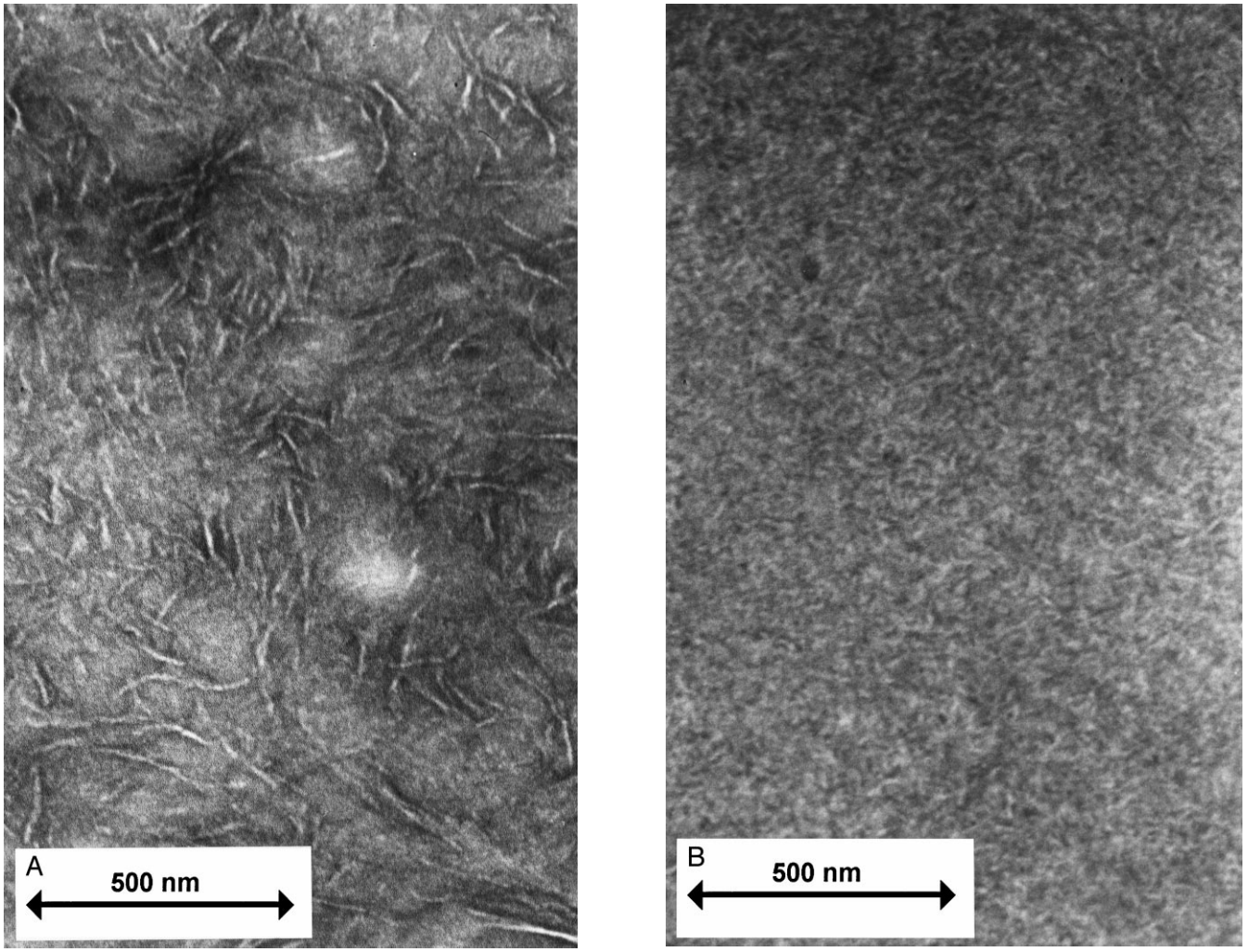

Figure 8 TEM micrographs of two homogeneous ethylene–propylene copolymers after staining with chlorosulphonic acid vapour at room temperature: (A) lamellar base morphology for EP 207 and additional granular structures; (B) granular base morphology in the case of EP 203

storage at room temperature have to do with this. Furthermore, annealing occurs during isothermal stays at *any* temperature. This is readily observable if the sample is subsequently cooled for a short while and then heated. The heat capacity derived from the heating curve will then be smaller below the annealing temperature and higher above the annealing temperature; around the annealing temperature the $c_p(T)$ curve assumes the shape of a rotated S, while the heating curve without annealing has the usual shape (no S). The nature of the annealing process can only be guessed: the effects involved are very subtle and cannot (yet) be directly monitored via morphological techniques. In the crystallinity curves in *Figure 6* the annealing is visible as a dip in the curves just above room temperature.

Figure 7 shows crystallinity curves derived from d.s.c. heat capacity measurements and from WAXS synchrotron measurements for the homogeneous EP copolymer EP 207. The curves were measured in cooling and in heating and cover the entire relevant temperature range. The WAXS measurements show clearly observable orthorhombic 110 and 200 reflections, of which the 110 reflections served as a basis for calculating the crystallinity. The d.s.c. and WAXS measurements are in good agreement as far as the temperature axis is concerned: the differences are probably due to calibration differences and to thermal lag of the oven used in the synchrotron set-up. The crystallinity continuously changes in the entire temperature range above the glass transition, that is, above approx. −30°C.

SAXS synchrotron measurements also yield relevant information about the copolymers discussed here. The intensity curves $I(q,T)$ always show a correlation maximum. Whether or not this can be used for calculating a long period and the thicknesses of the crystallites, the amorphous layer and the transition layer depends on the detailed morphology. Only if this is known, e.g. on the basis of TEM micrographs, can it be ascertained whether analysis according to the 'direct method' and/or via the one-dimensional correlation function or Lorentz correction is possible. In this connection it is important to know whether or not lamellae are present; whether they are sufficiently large; whether there are stacks in which the lamellae are ordered parallel, etc. In the case of EP 207 the long periods in cooling and heating vary between approx. 11 nm (at the onset of crystallization and the end of melting) up to approx. 8.5 nm at the glass transition. Between the glass transition and approx. 30°C the curves coincide, which is in accordance with the d.s.c. and WAXS measurements.

TEM micrographs of the morphology are indispensable in interpreting the long period. However, obtaining this information is far from easy. In order for a good contrast to be achieved between the crystalline and amorphous phases the amorphous phase needs to be stained. In the case of

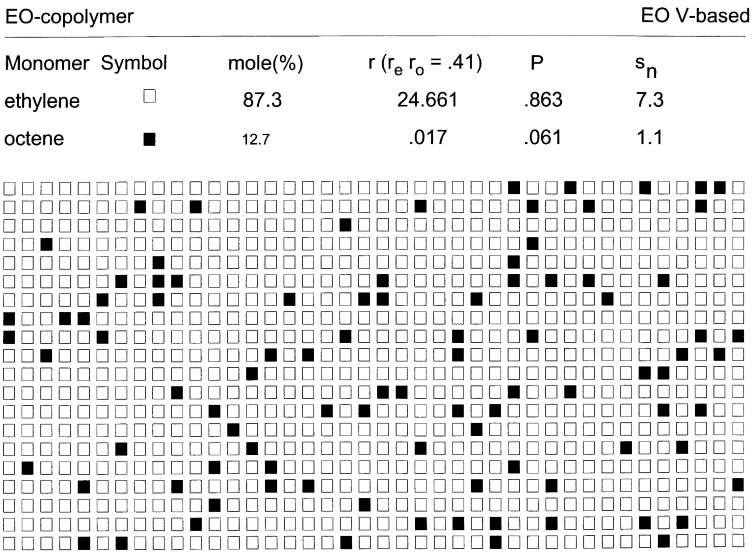

Figure 9 Simulation of the chain structure of the vanadium-based homogeneous ethylene-1-octene copolymer with $X_e = 88.5\%$. The chain is constructed by linking the end of each line to the beginning of the next line. Copolymer presentation of the succession of ethylene and 1-octene units. $P_{ee} = 0.863$ and $P_{oo} = 0.061$ are chain propagation probabilities: s_n is the number-average sequence length

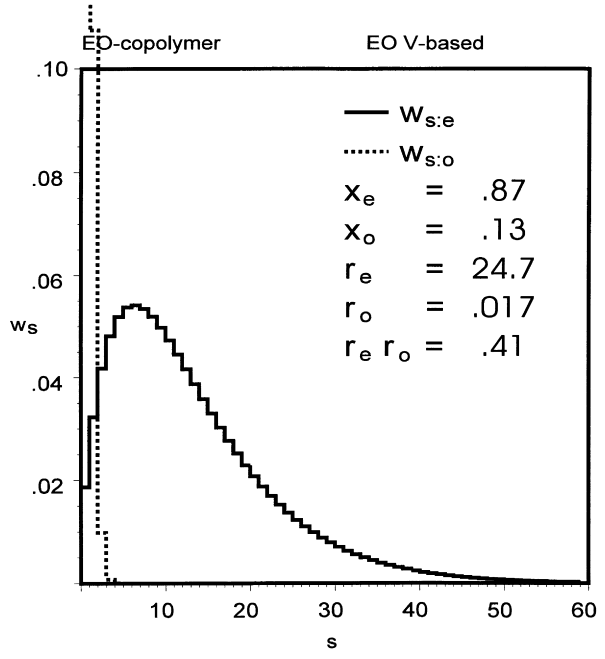

Figure 10 Ethylene, $w_{s:e}$, and 1-octene, $w_{s:o}$, sequence length distributions for the vanadium-based homogeneous ethylene-1-octene copolymer

the copolymers discussed here, the temperature at which staining and fixation takes place is important because—depending on the ethylene content—crystallization and melting may continue into the glass transition region. As the activity of the staining agents used decreases with decreasing temperature, staining at temperatures lower than 0°C is hardly ever practised because the staining times would be prohibitively long. At the moment, staining at room temperature, let alone at 0°C, is only just feasible.

Figure 8 shows TEM micrographs for EP 207 and EP 203, ethylene–propylene copolymers which contain ethylene mole percentages of 89.4 and 82.6%, respectively. The density at room temperature of EP 207 is 896 kg/m^3. The density of EP 203 was not measured but is definitely lower than 870 kg/m^3, so with this polymer we anticipate the discussion in the following sections. It is remarkable that EP 207 shows a lamellar base morphology (lamellae having a thickness of approx. 9 nm, with lengths of at least 250 nm being visible) with additional granular structures while in EP 203 no lamellae are visible: the base morphology is granular (the dimensions of the granular structures being 6–12 nm). TEM results obtained for other copolymers (ethylene-1-butene and ethylene-1-octene) support our conclusion that as the comonomer content increases the lateral dimensions of the lamellae decrease until granular structures remain[3,47,50]. Also, the spherulitic superstructure originally present disappears. The changes in morphology are found to be continuous as a function of the comonomer content[50].

At the same time, in WAXS measurements on the EP copolymers (and on homogeneous copolymers in general) the crystal reflections become weaker as the comonomer content increases, to the point where they virtually disappear. At a density of approx. 870 kg/m^3 the reflections are so weak that, for example, the crystallinity can no longer be calculated on the basis of WAXS measurements. There is of course a connection between the disappearance of the reflections and the continuous change to ever smaller dimensions as revealed by the TEM micrographs. Apparently, owing to the increasingly smaller dimensions in combination with imperfections in the crystalline structures, constructive interference is no longer possible, which explains the absence of crystal reflections.

This means that for homogeneous ethylene copolymers having densities of less than approx. 870 kg/m^3 (or having a mass crystallinity of less than about 12%: this limit is rather arbitrary and depends on the microstructure) WAXS can no longer be used because there are no reflections and TEM can no longer be used because of staining problems at low temperatures and because of the increasingly smaller structures.

It would seem plausible that samples like EP 203 and copolymers with higher comonomer contents are no longer semi-crystalline or crystallizable, but this is not the case, as will be demonstrated in the next section. However, crystallization and melting do take place at ever lower

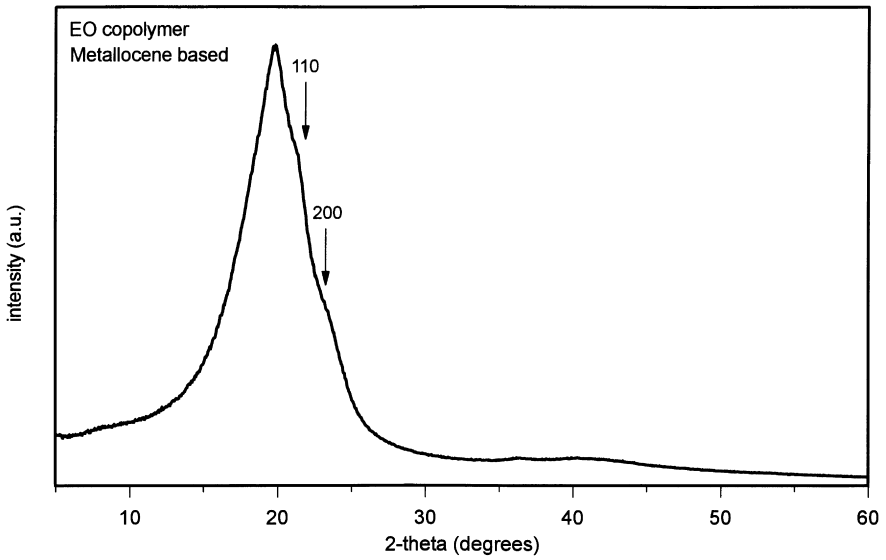

Figure 11 WAXS curve for the metallocene-based homogeneous ethylene-1-octene copolymer after cooling from 150°C to room temperature at 20°C/min

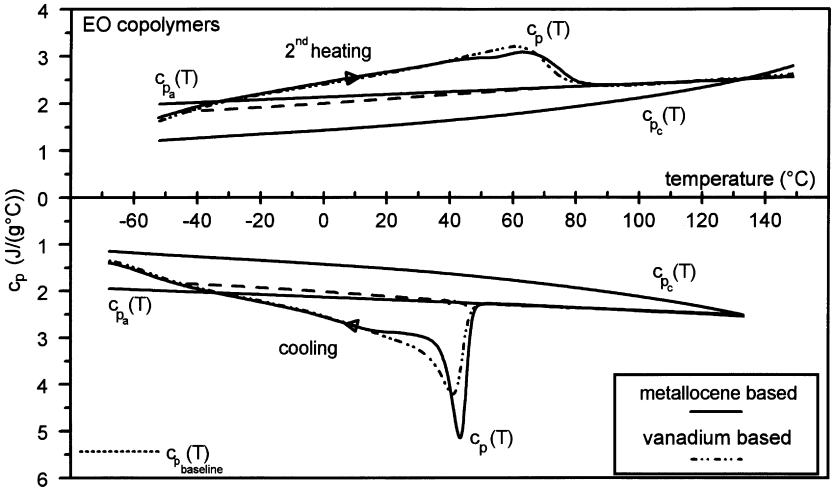

Figure 12 D.s.c. continuous specific heat capacity curves, $c_p(T)$, at 20°C/min; the reference curves, $c_{p_a}(T)$ and $c_{p_c}(T)$, and the baseline curves, $c_{p_b}(T)$ (— — —), for two homogeneous ethylene-1-octene copolymers produced with the aid of different catalyst systems. Cooling curves (downwards) and subsequent heating curves (upwards)

temperatures until the glass transition is reached, which prevents further crystallization.

At the borderline: homogeneous copolymers having a density of about 870 kg/m^3. This section describes the chain microstructure as well as the crystallization and melting behaviour of two homogeneous ethylene-1-octene copolymers having a density of approx. 870 kg/m^3. Both EO copolymers are homogeneous, but the catalysts used are different, namely metallocene-[3] and vanadium-based[51,52]. In *Figure 9* the chain microstructure of the vanadium-based copolymer is simulated and *Figure 10* shows the corresponding ethylene and octene sequence length distributions. For the calculation of the set of reactivity ratios the ^{13}C NMR based results were fitted with a specially developed 'degenerated terpolymer' model which takes into account that during polymerization the octene units may be incorporated into the chain both 'normally' and 'invertedly'[53–55]. Since this fine structure is of no relevance to the crystallization behaviour, only copolymer plots are given here. These plots were obtained by calculating 'pseudo' copolymer reactivity values. The product of r_e and r_o having a value of 0.41, the 'copolymerization' statistics are intermediate between alternating and random. The copolymer contains a wide range of sequence lengths, the longest being approx. 50. The octene units mainly occur isolated or in pairs.

The WAXS curve, measured at room temperature, in *Figure 11* shows hardly any crystal reflections[56], which is due to the lack of constructive interference. As noted earlier, this can only be due to the small dimensions of the crystalline structures, probably in combination with the imperfection of these structures. This is confirmed by TEM pictures obtained after staining at room temperature, which show that both copolymers have a granular base morphology with additional lamellar structures. However, the lamellae are thin, short and very irregularly shaped. These lamellae (which are probably formed by the longer ethylene sequences) no doubt cause the weak crystal reflections in the WAXS curve.

All this does not mean that the copolymers cannot crystallize. They can, as appears from *Figure 12*, in which

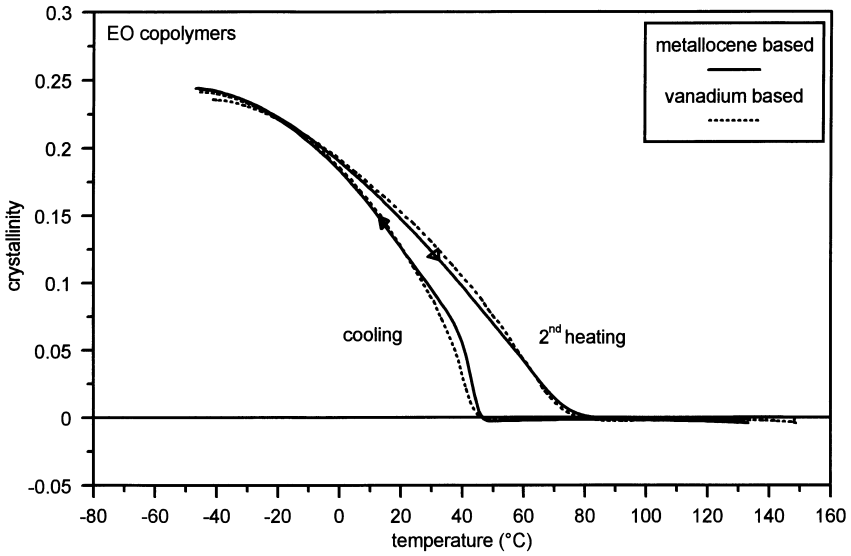

Figure 13 Enthalpy-based mass crystallinity curves for cooling and heating as obtained from *Figure 12*

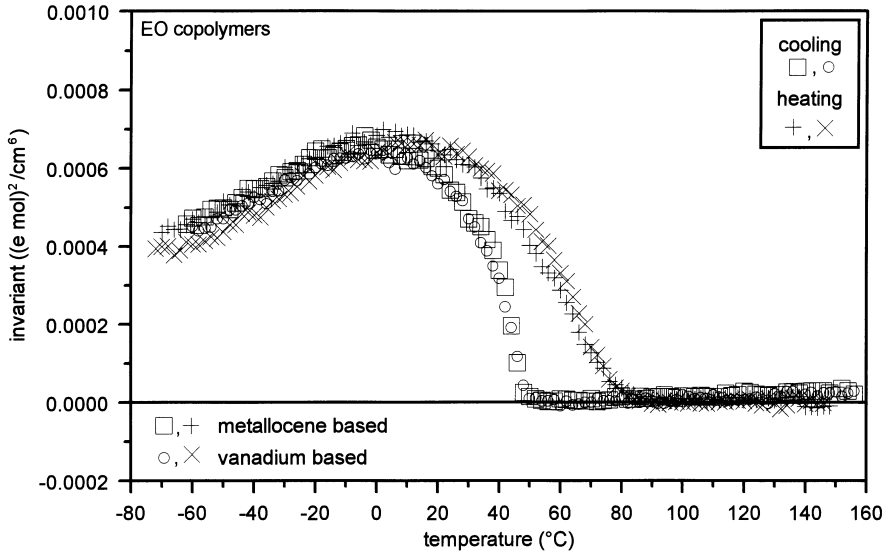

Figure 14 SAXS invariant curves for cooling and subsequent heating at 20°C/min for two homogeneous ethylene-1-octene copolymers, produced with the aid of different catalyst systems

crystallization and melting were recorded by means of d.s.c. heat capacity measurements. In the cooling run, crystallization starts at around 50°C and does not stop until the glass transition is reached, which starts at about −50°C. In the heating run first a devitrification takes place, upon which the copolymers melt until the melting end temperature of about 90°C is reached.

The crystallinities can be obtained by integrating the c_p measurements and comparing the results with the temperature-dependent enthalpy reference values in the two-phase model. *Figure 13* shows the temperature-dependent crystallinities. At room temperature these lie around 14%, the maximum crystallinity at the glass transition being slightly less than 25%. Here, too, it can be seen that during storage at temperatures near room temperature annealing is likely to occur. In short: contrary to what WAXS suggests, the copolymers are definitely semi-crystalline.

Despite the negative WAXS results, it is an X-ray technique which confirms this conclusion: SAXS appears to be an excellent technique for recording crystallization and melting phenomena for all copolymers, just as d.s.c. is. *Figure 14* shows an example for the EO copolymers. The onset of crystallization and the end of melting based on the SAXS invariant values as a function of temperature agree well with the d.s.c. results, the thermal history being the same. In the two-phase model the maxima in the curve are explained qualitatively as being due to the opposing effects of the crystallinity and density terms as functions of the temperature. However, as the comonomer content increases, it appears to become increasingly more difficult to find quantitative agreement between the measured and calculated values. This will be discussed in the next section.

It is remarkable that the crystallization and melting behaviour and the corresponding morphology of the two homogeneous ethylene-1-octene copolymers are comparable in every respect. This implies that the ethylene sequence length distributions can hardly be different, despite the fact that the chain microstructures are based on essentially different catalysts.

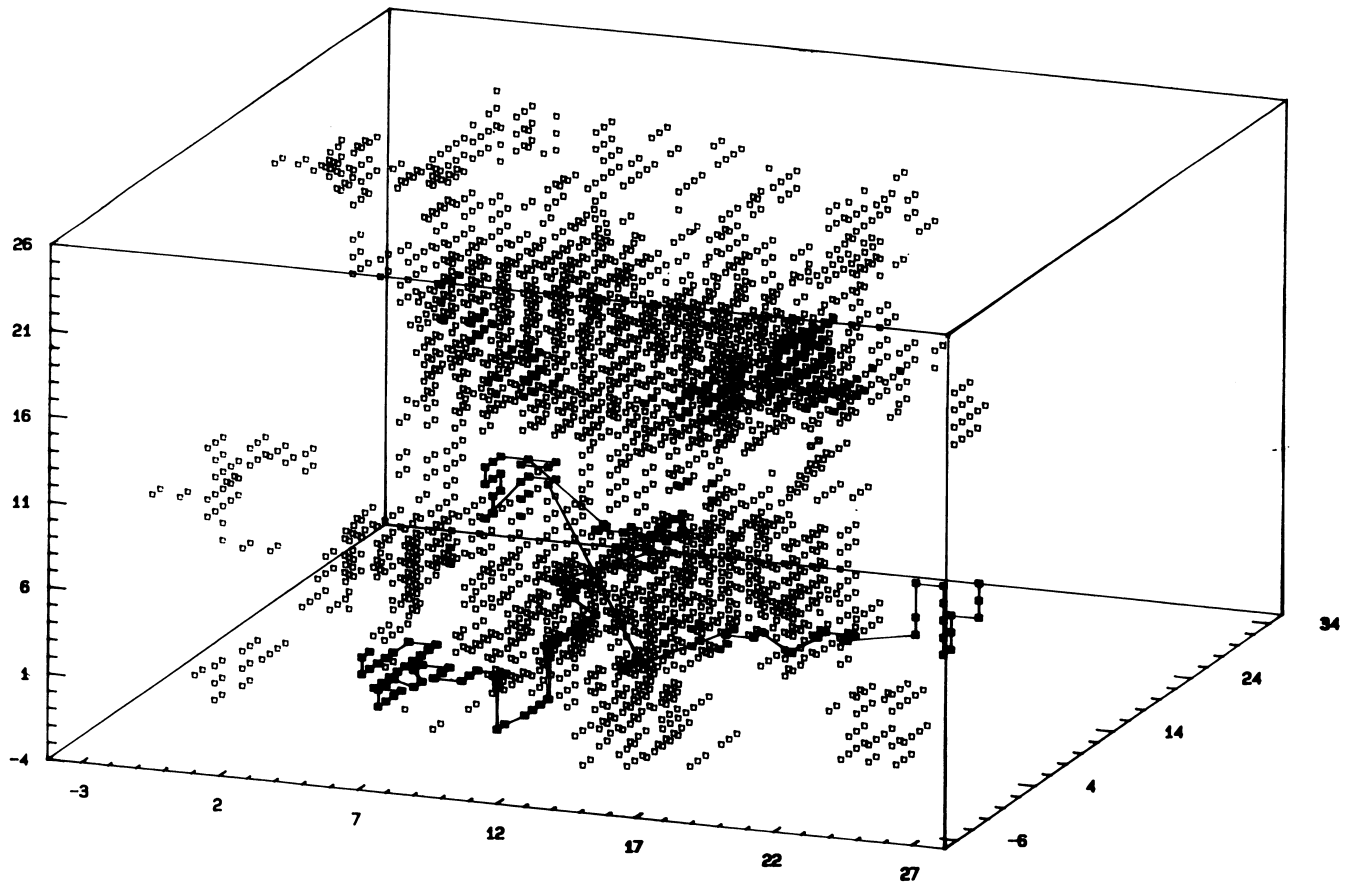

Figure 15 Monte Carlo simulation of the spatial arrangement of crystallized ethylene units belonging to 20 chains of a homogeneous ethylene–propylene copolymer, each consisting of 400 monomer units. The mole percentage ethylene of the copolymer is 65%. A single copolymer chain is highlighted, for which the phantom amorphous chain parts are represented by straight lines

Low order in homogeneous copolymers having densities below about 870 kg/m^3. It has been suggested that the cause of the discrepancy found between the measured and calculated SAXS invariant values for the copolymers might be that the density value for the crystalline phase in the two-phase model is too high. This density, for which the temperature-dependent values according to Swan[57] and Wilski[58,59] were used, is the density of a perfect orthorhombic crystal. As the crystallites become smaller according to TEM micrographs (and according to WAXS probably also increasingly imperfect), it may be expected that with increasing comonomer content the density of the crystalline phase will be lower than that of a perfect crystal with large dimensions. When a lower density is used in the calculations, the measured and calculated values of the EO copolymers discussed here can indeed be brought into line with each other.

The assumption that with increasing comonomer content the crystallites become ever smaller and less perfect and that, consequently, the density of the crystalline phase decreases is also made plausible by Monte Carlo simulations[60]. Simulations for copolymers with very high comonomer contents showed a fractal-like crystal growth. *Figure 15* shows the result of such a simulation in the form of a 3D-morphology. Only crystallized ethylene sequences are shown, the non-crystallized chain sections being assumed to be phantom. The morphology suggests a fairly open structure of 'loosely packed ethylene sequences' in which there are no longer any crystallites in the usual sense of the word. Regions and boundaries are difficult to indicate, which is why we prefer to use the term 'clusters' to refer to the form in which the loosely packed ethylene sequences are organized. The simulation gives a qualitative explanation for the measurements. D.s.c. measures the enthalpy changes during crystallization; the crystallized ethylene sequences will produce no constructive interference in WAXS whereas the density fluctuations are sufficiently large to produce scattering in SAXS. It is also conceivable that the density in the clusters is lower than that of a perfect orthorhombic crystal. An indication of this is that the simulation shows that the average coordination (perpendicular to the ethylene sequence) of a crystallized ethylene unit consists of three crystallized ethylene units, as against four in the case of a perfect crystal lattice. The loosely packed nature of the ethylene sequences will also give rise to a difference between the crystallinity based on the *enthalpy change* and the crystallinity based on the *number* of crystallized units: the latter crystallinity exceeds the former by a factor of almost 2. Since the simulations show that the average coordination with about three units is independent of the crystallization conditions and the crystallinity, it is reasonable to assume that the crystal growth is of a fractal nature. Incidentally, the simulation produced several other interesting results. For example, at a fixed degree of supercooling as a function of time there was always a dynamic equilibrium: metastable crystallized units were found to melt again, only to return later in more stable structures. Also, hysteresis between crystallization and melting was found. Clearly, such a crystallization model is far removed from Flory's equilibrium theory; it is much closer to models

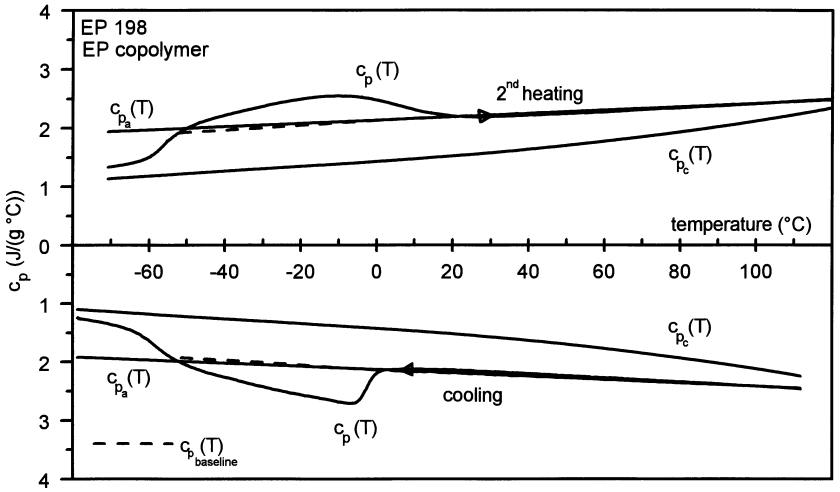

Figure 16 D.s.c. continuous specific heat capacity curves, $c_p(T)$, at 10°C/min for EP 198 obtained in cooling (downwards) and subsequent heating (upwards) between −80 and 120°C; the reference curves, $c_{p_a}(T)$ and $c_{p_c}(T)$ and the baseline curves, $c_{p_b}(T)$ (— — —)

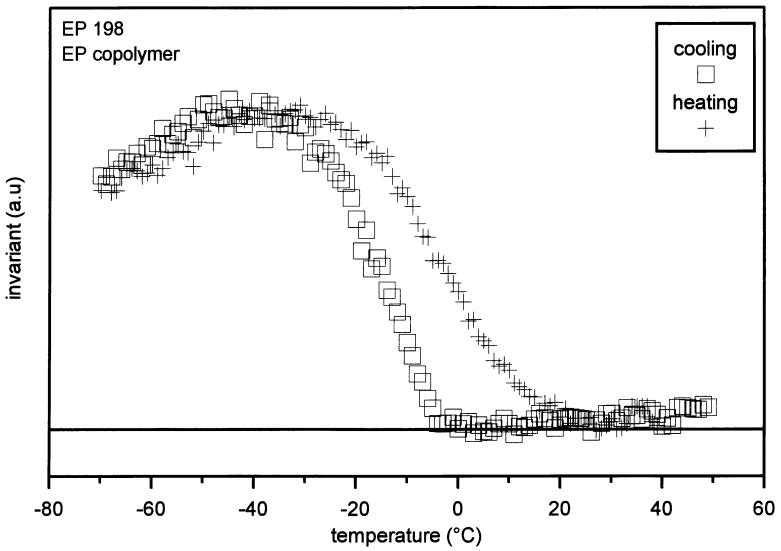

Figure 17 SAXS invariant curves for cooling and subsequent heating at 20°C/min between approx. −70°C and approx. 50°C for EP 198

involving hindered crystallization, such as Kilian's model[34] or, at the extreme end, Wunderlich's 'cold crystallization' model[61], in which in a crystallization process only neighbouring sequences can find each other. This limit situation is conceivable for the copolymers under review here, because these copolymers crystallize closer and closer to the glass transition temperature as the comonomer content increases.

Figure 16 shows the crystallization of an EP copolymer containing about 69 mol% ethylene, with a number-average ethylene sequence length of about 3 and an ethylene sequence length distribution in which the longest sequences are about 20 units long. Propylene sequences with lengths of up to 6 occur. The d.s.c. heat capacity measurements show that crystallization is hindered to a considerable degree by the propylene units, causing the copolymer to crystallize below about 0°C in the cooling run. Crystallization continues into the glass transition; upon heating devitrification occurs, followed by melting up to about 20°C. The measurement can readily be carried out and is consistent with the c_p reference curves.

A density measurement at room temperature would yield the density of the melt, which explains why copolymers and rubbers of the type discussed here are often thought to be amorphous. The experimental problems with this type of copolymers are mounting in several respects, not only because measurements have to be taken at temperatures below room temperature but also because several experimental methods have not been fully developed yet. TEM, for example, gives no results because the staining would have to be carried out at low temperatures, which would take much too long with the staining agents currently available, such as chlorosulphonic acid and ruthenium tetroxide. Nor is it possible at present to carry out crystallization/dissolution fractionations with the aid of TREF, for example, to verify the homogeneity of comonomer incorporation.

Down to −70°C, WAXS measurements on the copolymer show no crystal reflection whatsoever. Again, SAXS monitors the crystallization and melting phenomena well, see *Figure 17* which includes the invariants as functions of temperature. The onset of crystallization, the end of melting and the hysteresis are in agreement with the d.s.c. measurements. In addition, the maxima observed earlier are present in this case, too.

Finally, it should be noted that the ethylene sequence

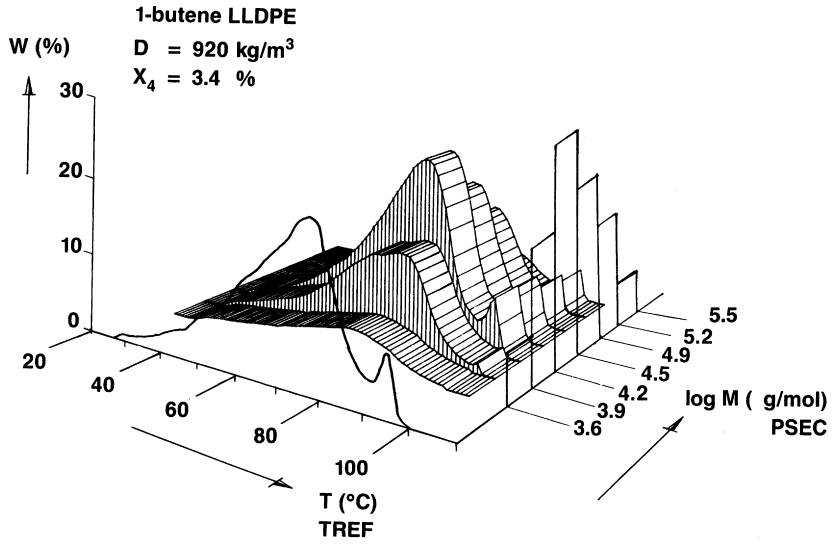

Figure 18 Cross-fractionation of a heterogeneous 1-butene LLDPE via analytical temperature rising elution fractionation after preparative size exclusion chromatography fractionation. In addition, the mathematical sums of the separate values for the fractions are indicated in two directions (arbitrary scales)

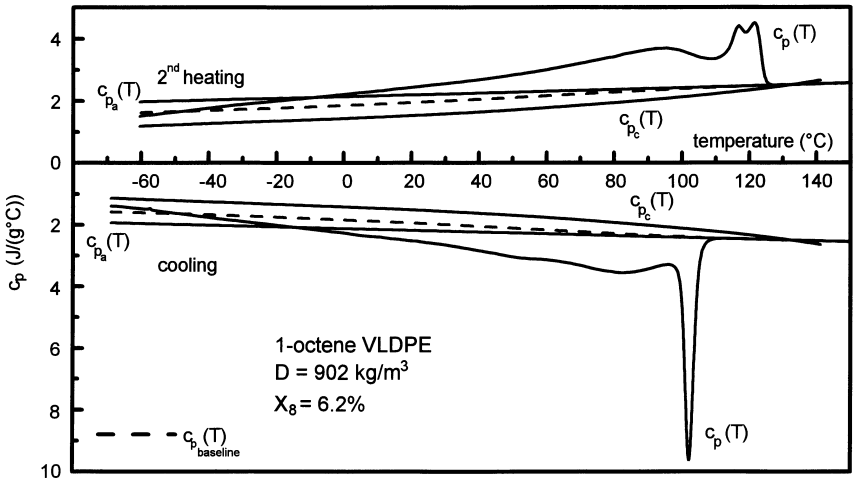

Figure 19 D.s.c. continuous specific heat capacity curves, $c_p(T)$, at 10°C/min; the reference curves, $c_{p_a}(T)$ and $c_{p_c}(T)$, and the baseline curves, $c_{p_b}(T)$ (— — —), for a heterogeneous 1-octene VLDPE polymerized using a Ziegler–Natta catalyst. Cooling curves (downwards) and subsequent heating curves (upwards)

length distribution in the homogeneous copolymers gives rise to broad crystallization and melting temperature distributions. It is therefore not surprising that in one and the same sample different morphologies can occur side by side[62], as was observed earlier for the EP copolymers (*Figure 8*: lamellar and granular structures) and was also found for the EO copolymers discussed here[47], see note to *Figure 11*.

Heterogeneous copolymers

We shall now pay some attention to copolymers which are heterogeneous because the catalyst used in their preparation had at least two active sites. In such cases one may expect the corresponding ethylene sequence length distributions to give rise to a multistep crystallization, resulting in several crystal thickness populations reflected in a multipeaked melting point distribution, see the classification according to *Figure 1*. The LLDPE and VLDPE discussed here are intermolecularly heterogeneous[63,64], that is, the heterogeneity is mainly between chains. By this we mean that chains containing many comonomer units and chains containing few comonomer units can have the same length. A characteristic feature of the Ziegler–Natta catalysts used is that *on average* the comonomer content increases with decreasing chain length. 'On average', because in all chain length classes, even the longest and the shortest ones, there are still chains with a high comonomer content as well as chains with a low comonomer content. This was revealed by extensive cross-fractionation experiments in which the fractions were separated according to chain length as well as crystallizability (ethylene sequence length; comonomer content)[65]. The fact that the heterogeneity is essentially intermolecular was demonstrated by crystallization/dissolution fractionations. The simple fact that molecules with narrow comonomer distributions could be isolated proves that the heterogeneity is intermolecular, not intramolecular.

The most straightforward cross-fractionation method is to first separate according to length and then separate the fractions according to crystallizability. This was done with the aid of, among other things, direct extraction and crystallization/dissolution fractionation. *Figure 18* shows a different combination as applied to a 1-butene LLDPE having a density of 920 kg/m^3: preparative size exclusion

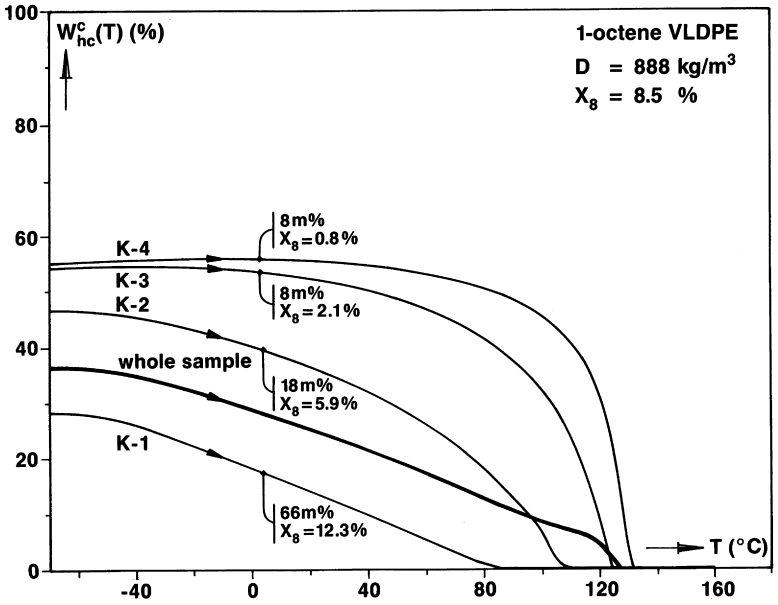

Figure 20 Enthalpy-based mass crystallinity heating curves based on d.s.c. heat capacity measurements at 10°C/min for a heterogeneous 1-octene VLDPE: whole sample and fractions thereof as obtained by crystallization/dissolution fractionation

chromatography (PSEC) followed by analytical temperature rising elution fractionation (ATREF). In the first step fractions are obtained which have narrow molar mass distributions. By performing TREF on these fractions one can then obtain information about the dissolution behaviour after crystallization in solution. It can clearly be seen that the dissolution curves have two peaks, with the highest-melting material mainly being present in the high-molar-mass part of the copolymer. Summation of the TREF curves yields the two-peaked dissolution curve corresponding to the TREF curve of the product started from. The presence of multiple peaks is characteristic of LLDPE and VLDPE and virtually always characterizes the d.s.c. curves. A single peak is obtained only upon heating after cooling at extremely high rates, probably due to promoted co-crystallization. In d.s.c. measurements, at certain combinations of cooling and heating rates the highest melting peak is split up into two sub-peaks due to recrystallization. This can occur in TREF as well, despite the fact that in TREF very low cooling rates are used, precisely to avoid such 'kinetic influences'. There are also differences between the results of TREF and d.s.c. measurements. In d.s.c., the lowest-melting peak is much smaller than in TREF, although the TREF analysis shows that this peak is produced by a considerable amount of material (compared with the amount of material responsible for the highest melting peak). However, experiments in which the sample was crystallized in the d.s.c. apparatus in solution and then dissolved also show a considerable increase in the lowest-melting peak relative to the highest-melting peak. This leads to the conclusion that a solvent facilitates the crystallization of branched molecules to a considerable degree because hindrances such as entanglements, which have a major effect on crystallization from the melt, occur to a lesser degree. This does not mean that the molecules no longer influence one another; after all, a considerable number of molecules crystallize at a concentration which is higher than the overlap concentration. So it is not surprising that experiments have shown that even in crystallization from a solution, and even in TREF, effective separation of components which differ only slightly in terms of ethylene sequence length is prevented by co-crystallization[66].

The morphology of LLDPEs as revealed by TEM shows a characteristic picture[67], see *Figure 21a*. Besides lamellae having a length of several microns, which build the spherulitic superstructure that fills the space soon after crystallization commences, at lower temperatures smaller and slightly thinner lamellae are formed in between the longer ones. This means that the two-step crystallization is directly reflected in a bimodal morphology.

Figure 19 shows that a 1-octene VLDPE having a density at room temperature of 902 kg/m^3 also has two-peaked crystallization and melting temperature distributions. The crystallization takes place in two stages and for the least copolymerized chains it starts above 110°C. The second crystallization peak has its maximum around 83°C and is caused by the more heavily copolymerized chains. Vitrification takes place at the lowest temperatures in about the same temperature range as in the case of homogeneous copolymers having the same density at room temperature. The heating curves also show two peaks, *viz*. at around 93°C and 115°C. These correspond to the crystallization peaks at around 83 and 102°C, respectively. The peak at about 120°C is the result of recrystallization of the peak at 115°C. This concerns the chains with the lowest comonomer contents. Although these are mostly the longer chains, this type of chain can be found throughout the entire molar mass distribution, including the shortest chains. A remarkable observation in the c_p curve is that crystallization takes place up to the glass transition region, and melting takes place from the glass transition region onwards. This means the crystallization and melting ranges are extremely broad: about 160 and 175°C, respectively. It is virtually impossible to carry out this kind of measurement quantitatively without making special provisions, such as subtraction of empty pan measurements and extra temperature stabilization of the d.s.c. apparatus to avoid drift during the measurements.

The extremely broad crystallization range also means that during crystallization in cooling various different crystallization mechanisms are operative. At the highest

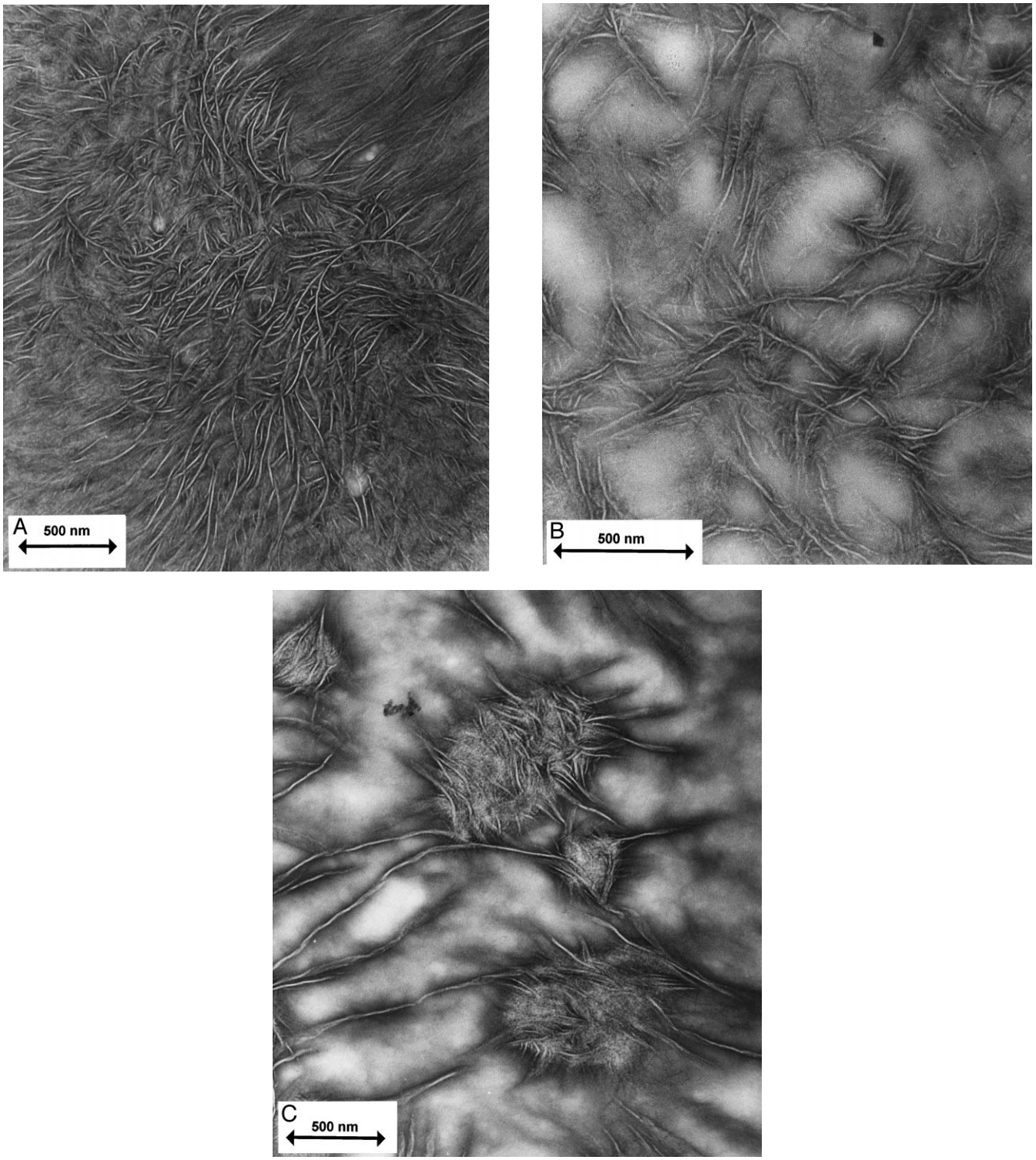

Figure 21 TEM micrographs (obtained after staining with chlorosulphonic acid vapour) of heterogeneous ethylene copolymers: an 1-octene LLDPE of density 919 kg/m^3 (A) and two 1-octene VLDPEs of densities 902 kg/m^3 (B) and 888 kg/m^3 (C)

temperatures folded-chain crystallization in lamellar crystallites is to be expected, but as the temperature decreases the lateral dimensions of the lamellae will decrease to the point where folded-chain crystallization occurs in granular crystallites as discussed earlier. The crystallization mechanisms and the resulting morphologies at still lower temperatures are not known. As far as this temperature range is concerned one has to rely on theoretical considerations; assumptions (bundled sequences in fringed micelles[10]); the simulation discussed earlier (clusters of loosely packed ethylene sequences) and finally the 'cold crystallization' concept in the case of crystallization near or from the glass transition region. The crystallization mechanisms and the resulting morphologies of ethylene-based copolymers in the temperature range between the glass transition region and, say, 60°C are relatively uncharted territory not only from an experimental point of view; from a theoretical point of view, too, this is a blank region because hardly any concepts have been developed which are useful in the sense that they take into account hindrances during crystallization

which are responsible for the high degree of kinetic determinacy of nucleation and growth and which make a high degree of metastability unavoidable.

Clearly, in heterogeneous copolymers such as VLDPE a wide range of morphologies can be expected. *Figure 21b* shows a part of the morphology, namely the part made visible by staining for 64 h with chlorosulphonic acid in the vapour phase at room temperature. In this sample, too, there are lamellae which right from the onset of crystallization start to build space-filling (irregularly shaped) spherulites with a diameter of about 20 μm via a radial orientation. It is difficult to establish exactly how long these lamellae are, as they twist with a period of about 1 μm. The TEM micrograph in the figure was made at a place where no orientation of lamellae occurred. Besides the longer lamellae, shorter lamellae can also be seen. In addition, there are many regions where nothing is to be seen. These could be regions where the lamellae lie 'flat on' so that there is no contrast between amorphous and crystalline material. However, this is at best a partial explanation, as the figure shows not only lamellae which provide a high contrast because they are positioned 'edge on' but even many lamellae which are positioned 'flat on'. As a result, even the twisting can be observed very well. So the fact that in the 'white' regions nothing can be seen must be due to several causes, such as material still being in the molten state at the staining temperature; structures being positioned 'flat on' and possibly also crystallites being destroyed by the staining procedure. A significant detail in this connection is that in our experience different aspects of the morphology can be made visible by using different staining times. We tentatively conclude that this VLDPE has a co-continuous morphology made up of two kinds of material: on the one hand material with a low to moderate degree of branching (as in LLDPE), whose morphology is visible in the figure, and on the other hand heavily copolymerized material which is still in the molten state at the staining temperature. In qualitative terms this picture is in agreement with the results of previous studies in which the heavily copolymerized material proved to be partially extractable[68].

The effects described above are much more pronounced in the case of the VLDPE having a still lower density at room temperature (888 kg/m^3). The intermolecularly heterogeneous nature of this copolymer appears from the fact that by means of crystallization/dissolution fractionation it has been possible to isolate fractions having narrow comonomer distributions. This is apparent from c_p measurements in heating, of which the resulting crystallinity curves are given in *Figure 20* together with the curve for the product started from. While the original sample has an average octene content of 8.5 mol%, at the highest temperatures fractions are obtained which have 1-octene contents of 0.8 mol% (8% by mass); 2.1 mol% (8% by mass) and 5.9 mol% (18% by mass). At room temperature the greater part of the material (66% by mass) remained in solution. This largest fraction, which still has an *average* 1-octene content of 12.3%, can no doubt be split up further into fractions with higher octene contents if the fractionations could be carried out at low temperatures. The figure shows that an extremely broad distribution of octene contents is present in the sample, which causes the extremely broad crystallization and melting ranges. So the sample is a blend of slightly to very heavily copolymerized chains made in the reactor using a catalyst with at least two active sites.

The morphology is likewise complex, see *Figure 21c*. The phase with a lamellar morphology which in the VLDPE with a density of 902 kg/m^3 was still the continuous phase is now the dispersed phase. We have introduced the term 'compact semi-crystalline domains' (CSDs) to refer to the sometimes spherical structures which are conspicuous entities in an otherwise amorphous matrix. Another interesting finding is that the CSDs are interconnected by long, isolated lamellae. Apparently, via segregation through crystallization a dispersed phase is formed consisting of material with a relatively low to moderate degree of branching (as in LLDPE), whose morphology is visible in the figure in a matrix formed by material which is heavily copolymerized and which is still molten at the staining temperature. As the TEM micrograph in *Figure 21c* was taken after staining with chlorosulphonic acid in the vapour phase at 45°C, this means that no direct morphological information is available for this sample in the temperature range between about −40 and 45°C. The amount of material involved is considerable, as is also apparent from the fractionation results in *Figure 20*. Not only is a large fraction still dissolved at room temperature; the crystallinity at the glass transition is still more than 15% higher than the crystallinity of 20% measured at room temperature.

CONCLUSIONS

The polyethylenes discussed here illustrate the very large variation in structure and properties resulting from many years of development work. For all types, the chain macrostructure and microstructure and the thermal history have a strong influence on the crystallization and melting behaviour and the morphology.

In all polyethylenes, a considerable degree of reorganization is likely to occur under normal experimental conditions, not only during heating but also during cooling. At high degrees of short chain branching this reorganization is reduced but it does not disappear entirely.

As the comonomer content increases, the resulting shorter ethylene sequences cause the copolymer molecules to crystallize at lower and lower temperatures and in smaller and smaller, less and less perfect structures. As a result, these structures produce less and less WAXS crystal reflections.

With crystallization taking place at lower and lower temperatures, there comes a point where TEM can no longer be used because there are no staining agents available which are sufficiently active at sub-ambient temperatures. At these low temperatures it is also difficult to carry out crystallization/dissolution fractionations for determining the heterogeneity of comonomer incorporation. This explains why these fractionations have not been carried out so far.

D.s.c. and time-resolved SAXS can be used for all copolymers. They give detailed information and are in good agreement with each other as far as the onset of crystallization, the end of melting and hysteresis are concerned. However, there are no adequate morphology models available for interpreting the SAXS results. This holds in particular for the interpretation of the correlation maxima found in all copolymers, but also for the temperature-dependent invariants.

For virtually all samples the two-phase model is adequate and there is no reason to assume a third phase. However, it is essential that quantitative measurements be carried out. For d.s.c. this means heat capacity measurements and

evaluation using temperature-dependent enthalpy reference values for the amorphous and crystalline phases.

ACKNOWLEDGEMENTS

The authors would like to thank Ms S. Coolen and Mrs M. Walet for the TEM measurements.

REFERENCES

1. Mathot, V. B. F., Crystallization and melting of linear, branched and copolymerized polyethylenes as revealed by fractionation methods and DSC, in *New Advances in Polyolefins*, ed. T. C. Chung. Plenum Press, New York, 1994, p. 121.
2. Hosoda, S., Uemura, A., Shigematsu, Y., Yamamoto, I. and Kojima, K., *Stud. Surf. Sci. Catal.*, 1994, **89**, 365.
3. Hwang, Y.-C., Chum, S., Guerra, R. and Sehanobish, K., in *Antec '94 SPE Conf. Proc.*, Vol. III, 1994, p. 3414.
4. Mathot, V. B. F., The crystallization and melting region, in *Calorimetry and Thermal Analysis of Polymers*, ed. V. B. F. Mathot. Hanser Publishers, Munich, 1994, Chap. 9, p. 231.
5. Mathot, V. B. F. and Pijpers, M. F. J., *J. Therm. Anal.*, 1983, **28**, 349.
6. Bras, W., Derbyshire, G. E., Ryan, A. J., Mant, G. R., Felton, A., Lewis, R. A., Hall, C. J. and Greaves, G. N., *Nucl. Instrum. Meth. Phys. Res.*, 1993, **A326**, 587.
7. McFaddin, D. C., Russell, K. E., Gang , W. and Heyding, R. D., *J. Polym. Sci., Polym. Phys.*, 1993, **31**, 175.
8. Vonk, C. G., *J. Appl. Cryst.*, 1973, **6**, 148.
9. Keller, A., *Macromol. Symp.*, 1995, **98**, 1.
10. Wunderlich, B., *Macromolecular Physics*, Vol. 1, *Crystal Structure, Morphology, Defects*. Academic Press, New York, 1973.
11. Wunderlich, B., *Macromolecular Physics*, Vol. 2, *Crystal Nucleation, Growth, Annealing*. Academic Press, New York, 1976.
12. Keller, A., Hikosaka, M., Rastogi, S., Toda, A., Barham, P. J. and Goldbeck-Wood, G., *J. Mater. Sci.*, 1994, **29,** 2579.
13. Czornyj, G. and Wunderlich, B., *J. Polym. Sci., Polym. Phys.*, 1977, **15**, 1905.
14. Hager, N. E. Jr., *Rev. Sci. Instrum.*, 1964, **35**(5), 618.
15. Hager, N. E. Jr., *Rev. Sci. Instrum.*, 1972, **43**(8), 1116.
16. Domszy, R., in *Proc. Metallocenes '96*, Düsseldorf, 1996, p. 251.
17. Mathot, V. B. F. and Pijpers, M. F. J., *Polym. Bull.*, 1984, **11**, 297.
18. Hoffman, J. D., Frolen, L. J., Ross, G. S. and Lauritzen, J. I. Jr., *J. Res. Natl. Bur. Stand.*, 1975, **79A**, 671.
19. Hoffman, J. D., *Polymer*, 1983, **24**, 3.
20. Hoffman, J. D. and Weeks, J. J., *J. Res. Natl. Bur. Stand.*, 1962, **66A**, 13.
21. Wunderlich, B., *Macromolecular Physics*, Vol. 3, *Crystal Melting*. Academic Press, New York, 1980.
22. Chivers, R. A., Barham, P. J., Martinez-Salazar, J. and Keller, A. Jr., *J. Polym. Sci., Polym. Phys.*, 1982, **20**, 1717.
23. Barham, P. J., Chivers, R. A., Jarvis, D. A., Martinez-Salazar, J. and Keller, A., *J. Polym. Sci., Polym. Lett.*, 1981, **19**(11), 539.
24. Barham, P. J., Jarvis, D. A. and Keller, A., *J. Polym. Sci., Polym. Phys.*, 1982, **20**, 1733.
25. Martinez-Salazar, J., Barham, P. J. and Keller, A., *J. Mater. Sci.*, 1985, **20**, 1616.
26. Barham, P. J., Chivers, R. A., Keller, A., Martinez-Salazar, J. and Organ, S. J., *J. Mater. Sci.*, 1985, **20**, 1625.
27. Barham, P. J. and Keller, A., *J. Polym. Sci., Polym. Phys.*, 1989, **27**, 1029.
28. Albrecht, T. and Strobl, G., *Macromol.*, 1996, **29**, 783.
29. Hikosaka, M., *Polymer*, 1987, **28**, 1257.
30. Hikosaka, M., *Polymer*, 1990, **31**, 458.
31. Flory, P. J., *J. Chem. Phys.*, 1947, **15**(9), 684.
32. Flory, P. J., *Trans. Faraday Soc.*, 1955, **51**, 848.
33. Flory, P. J. and Mandelkern, L., *J. Polym. Sci.*, 1956, **21**, 345.
34. Kilian, H. G., in *Thermal Analysis and Calorimetry in Polymer Physics*, ed. V. B. F. Mathot, Special Issue of *Thermochim. Acta*, 1994, **238,** 113.
35. Murata, K. and Kobayashi, S., *Kobunshi Kagaku*, 1969, **26**, 536.
36. Hser, J.-H. and Carr, S.H., *Polym. Eng. Sci.*, 1979, **19**, 436.
37. Alamo, R. G. and Mandelkern, L., *Macromol.*, 1989, **22**, 1273.
38. Alamo, R. G., Chan, E. K. M., Mandelkern, L. and Voigt-Martin, I. G., *Macromol.*, 1992, **25**(24), 6381.
39. Alamo, R. G., Mandelkern, L., in *Thermal Analysis and Calorimetry in Polymer Physics*, ed. V. B. F. Mathot, Special Issue of *Thermochim. Acta*, 1994, **238,** 155.
40. Cheng, S. Z. D. and Wunderlich, B., *Macromol.*, 1988, **21**, 789.
41. Cheng, S. Z. D., Pan, R. and Wunderlich, B., *Makromol. Chem.*, 1988, **189**, 2443.
42. Mathot, V. B. F., Thermal characterization of states of matter, in *Calorimetry and Thermal Analysis of Polymers*, ed. V. B. F. Mathot. Hanser Publishers, Munich, 1994, Chap. 5, p. 105.
43. Peeters, M., Goderis, B., Vonk, C., Reynaers, H. and Mathot, V., *J. Polym. Sci., Polym. Phys.*, 1997, **35**, 2689.
44. Mathot, V. B. F. and Pijpers, M. F. J., *Thermochim. Acta*, 1989, **151**, 241.
45. Mathot, V. B. F. and Pijpers, M. F. J., *J. Appl. Polym. Sci.*, 1990, **39**(4), 979.
46. Mathot, V. B. F., Scherrenberg, R. L., Pijpers, T. F. J., Bras, W., in Special Issue in Honor of Professor Bernhard Wunderlich's 65th birthday, ed. E. A. Turi, *J. Therm. Anal.*, 1996, **46**(3–4), 681.
47. Mathot, V. B. F., Scherrenberg, R. L., Pijpers, M. F. J., Engelen, Y. M. T., Structure, crystallisation and morphology of homogeneous ethylene–propylene, ethylene-1-butene and ethylene-1-octene copolymers with high comonomer contents, in *New Trends In Polyolefin Science and Technology*, ed. S. Hosoda. Research Signpost, Trivandrum (India), 1996, 71.
48. Mathot, V. B. F., *Polymer*, 1984, **25**, 579.
49. Mathot, V. B. F., *Erratum. Polymer*, 1986, **27**, 969.
50. Bensason, S., Minick, J., Moet, A., Chum, S., Hiltner, A. and Baer, E., *J. Polym. Sci., Polym. Phys.*, 1996, **34**, 1301.
51. Mathot, V., Pijpers, M., Beulen, J., Graff, R., van der Velden, G., in *Proc. Second European Symposium on Thermal Analysis 1981 (ESTA-2)*, ed. D. Dollimore. Heyden, London, 1981, p. 264.
52. Hunter, B. K., Russell, K. E., Scammell, M. V. and Thompson, S. L., *J. Polym. Sci., Polym. Chem.*, 1984, **22**, 1383.
53. Mathot, V. B. F. and Fabrie, Ch. C. M., *J. Polym. Sci., Polym. Phys.*, 1990, **28**, 2487.
54. Mathot, V. B. F., Fabrie, Ch. C. M., Tiemersma-Thoone, G. P. J. M. and van der Velden, G. P. M., *J. Polym. Sci., Polym. Phys.*, 1990, **28**, 2509.
55. Mathot, V. B. F., Fabrie, Ch. C. M., Tiemersma-Thoone, G. P. J. M., van der Velden, G. P. M., in *Proc. Int. Rubber Conf. (IRC)*, Kyoto, 15–18 October 1985, p. 334.
56. McFaddin, D. C., Russell, K. E., Gang, W. and Heyding, R. D., *J. Polym. Sci., Polym. Phys.*, 1993, **31**, 175.
57. Swan, P. R., *J. Polym. Sci.*, 1962, **56**, 403.
58. Wilski, H., *Kunststoffe*, 1964, **54**, 10.
59. Wilski, H., *Kunststoffe*, 1964, **54**, 90.
60. van Ruiten, J., van Dieren, F., Mathot, V. B. F., in *Crystallization of Polymers*, ed. M. Dosière. NATO ASI-C Series on Mathematical and Physical Sciences, 1993, p. 481.
61. Wunderlich, B. J., *Chem. Phys.*, 1958, **29**(6), 1395.
62. Minick, J., Moet, A., Hiltner, A., Baer, E. and Chum, S. P., *J. Appl. Polym. Sci.*, 1995, **58**, 1371.
63. Mathot, V., in *Polycon '84 LLDPE*. The Plastics and Rubber Institute, London, 1984, p. 1.
64. Mathot, V. B. F., Schoffeleers, H. M., Brands, A. M. G. and Pijpers, M. F. J., in *Morphology of Polymers*, ed. B. Sedlaček. Walter de Gruyter and Co., Berlin, 1986, p. 363.
65. Defoor, F., Molecular, thermal and morphological characterization of narrowly branched fractions of 1-octene LLDPE. Ph.D. Thesis, Catholic University of Leuven, Belgium, 1992.
66. Steenbakkers-Menting, H. N. A. M., Chlorination of ultrahigh molecular weight polyethylene. Ph.D. Thesis, Technical University of Eindhoven, The Netherlands, 1995.
67. Hosoda, S., Kojima, K. and Furuta, M., *Makromol. Chem.*, 1986, **187**, 1501.
68. Deblieck, R. A. C. and Mathot, V. B. F., *J. Mater. Sci. Lett.*, 1988, **7**, 1276.